RSC Advances

REVIEW

View Article Online
View Journal | View Issue

Cite this: *RSC Adv.*, 2021, **11**, 18351

Potential carbon nanomaterials as additives for state-of-the-art Nafion electrolyte in proton-exchange membrane fuel cells: a concise review

Mohanraj Vinothkannan,[a] Ae Rhan Kim*[b] and Dong Jin Yoo*[ab]

Proton-exchange membrane fuel cells (PEMFCs) have received great attention as a potential alternative energy device for internal combustion engines due to their high conversion efficiency compared to other fuel cells. The main hindrance for the wide commercial adoption of PEMFCs is the high cost, low proton conductivity, and high fuel permeability of the state-of-the-art Nafion membrane. Typically, to improve the Nafion membrane, a wide range of strategies have been developed, in which efforts on the incorporation of carbon nanomaterial (CN)-based fillers are highly imperative. Even though many research endeavors have been achieved in relation to CN-based fillers applicable for Nafion, still their collective summary has rarely been reported. This review aims to outline the mechanisms involved in proton conduction in proton-exchange membranes (PEMs) and the significant requirements of PEMs for PEMFCs. This review also emphasizes the improvements achieved in the proton conductivity, fuel barrier properties, and PEMFC performance of Nafion membranes by incorporating carbon nanotubes, graphene oxide, and fullerene as additives.

Received 26th January 2021
Accepted 5th May 2021

DOI: 10.1039/d1ra00685a

rsc.li/rsc-advances

[a]*R&D Education Center for Whole Life Cycle R&D of Fuel Cell Systems, Jeonbuk National University, Jeonju, Jeollabuk-do 54896, Republic of Korea. E-mail: djyoo@jbnu.ac.kr*

[b]*Department of Life Science, Graduate School of Department of Energy Storage/Conversion Engineering, Hydrogen and Fuel Cell Research Center, Jeonbuk National University, Jeonju, Jeollabuk-do 54896, Republic of Korea. E-mail: kimaerhan@jbnu.ac.kr*

Dr Mohanraj Vinothkannan received his Master of Science degree in Chemistry from Madurai Kamaraj University, Tamilnadu, India in 2014. He then joined as a PhD student under the supervision of Prof. Dong Jin Yoo, the Department of Energy/Storage Conversion Engineering, Jeonbuk National University, Jeonju, South Korea. During his PhD, Dr Vinothkannan worked on proton-exchange membranes and electrocatalysts applicable for fuel cells. Dr Vinothkannan received his PhD degree in 2018. At present, he is working as a research assistant professor in the R&D Education Center for Whole Life Cycle R&D of Fuel Cell Systems (directed by Prof. Dong Jin Yoo), Jeonbuk National University, Jeonju, South Korea. His current research interest is in the development of carbon-based proton-exchange membranes for various energy conversion and storage devices.

Dr Ae Rhan Kim obtained her Master of Science and PhD degrees in 1989 and 1996, respectively, in Chemistry at Jeonbuk National University, Jeonju, South Korea. During her PhD, she worked on the Photo-addition Reaction of Quinones. She has continuously worked in the same institute as a research professor and lecture professor since 1997, concentrating on the synthesis of block copolymers and their application in proton-exchange membranes for fuel cells and solar cells. Also, she has worked as a head of the R&D Center for CANUTECH, Business Incubation Center of Jeonbuk National University, Jeonju, South Korea since 2012. At present, she is working as a research professor and lecture professor at the Department of Life Science, Graduate School of Department of Energy Storage/Conversion Engineering, Jeonbuk National University, Jeonju, South Korea. Her research interest is the development of potential hydrocarbon-based electrolytes for various energy storage and conversion devices.

1. Introduction

The ever-increasing utilization of existing non-renewable energy resources (oil, coal, and natural gas) leads to energy insecurity along with harmful impacts to the environment, which not only violate the green infrastructure but also perturb the regular activities around the globe.[1] Until now, ~90% of the world's energy is generated by the incineration of non-renewable energy resources.[2] There is now a push for the mankind to seek alternative energy production associated with renewable energy sources. Renewable energy sources, such as hydroelectric power, wood, biofuels, wind, waste, geothermal energy, and solar energy, already generate ~9% of the total world energy demand, as demonstrated in Fig. 1.[2,3] The utilization of renewable resources for energy generation is thus being increased in developed and developing countries. For instance, energy production from renewable energy sources increased to 64% during the period 2007–2017 in the European Union (EU), and it would be expected to exceed this in the future.[4] It must be noted that the major contribution to EU's renewable energy currently comes from hydropower, biofuels and wind. In 2017, their contribution was 11.4%, 42%, and 13.8%, respectively, of the whole energy production.[3,4] However, energy production from renewable energy resources highly relies on the earth's weather conditions. Besides, the production cost of renewable energy is higher compared to that from the existing fossil fuels owing to the sophisticated instrumentation needed with renewable energy.[5–7] Another efficient route to producing renewable energy is the development of energy conversion devices.[8,9] Among the diverse array of energy conversion devices, fuel cells, especially, proton-exchange membrane fuel cells (PEMFCs), which can transform chemical energy into electrical energy through electrochemical reactions, are being considered as promising alternatives to internal combustion engines due to their high conversion efficiency, quick start-up and shut-down times, extraordinary power density, and nondetectable emission of pollutant gases.[10–14] Based on the operating temperature and electrolytes used, fuel cells can be categorized as follows: PEMFCs, alkaline fuel cells, molten carbonate fuel cells, phosphoric acid fuel cells, and solid oxide fuel cells.[15–19] In the present review, only PEMFCs will be considered. The PEMFCs consist of end plates with a hydrogen (H_2), methanol, or oxygen (O_2) inlet and outlet, graphite flow plates, air-tightening gaskets, gas-diffusion layers, anode, cathode, and the proton-exchange membrane (PEM) (Fig. 2).[20–22] H_2, methanol, ethanol, or formic acid is widely exploited as fuels for the anode and O_2 or air is used as a fuel for the cathode. During the anode reaction, H_2, methanol, ethanol, or formic acid flows through the gas-diffusion layer and spreads to the catalyst layer, where the dissociation of two protons and two electrons occur.[23–25] The two electrons transfer through the external circuit and reach the cathode, while the two protons pass through the PEM to the cathode catalyst layer. The reaction of the anode is as follows.

$$H_2 \rightarrow 2H^+ + 2e^- \quad (1)$$

Likewise, during the cathode reaction, O_2 attains the catalyst layer through the gas-diffusion layer, where it combines with

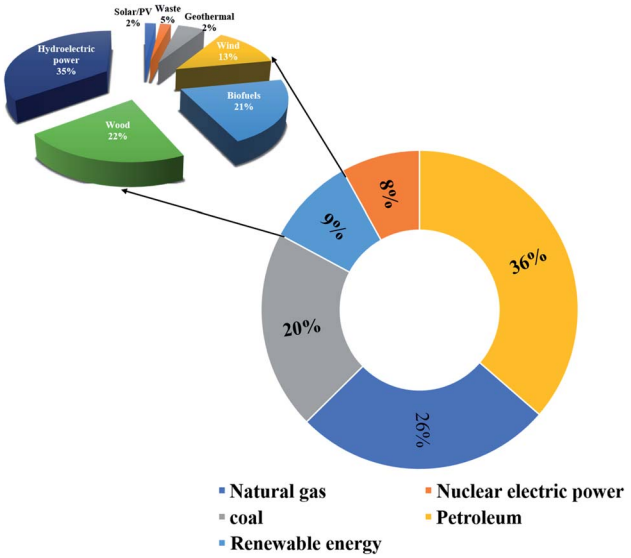

Fig. 1 Schematic breakdown of the global generation of energy.

Prof. Dong Jin Yoo is serving as a director of the Education Center for Whole Life Cycle R&D of Fuel Cell Systems and BK21, Educational Center for Hydrogen Energy Convergence Technology, Jeonbuk National University, Jeonju, South Korea. He received his PhD from the Jeonbuk National University, Jeonju, South Korea in 1991. Prof. Dong Jin Yoo worked as a post-doctoral fellow with Prof. Marc M. Greenberg at Colorado State University, USA up to 1995. Then, he worked as a professor at Seonam University, Jeollabuk-do, South Korea up to 2010. After that, he joined as a professor in the Department of Energy/Storage Conversion Engineering, Jeonbuk National University, Jeonju, South Korea on 2011. He has published about 198 research articles in various reputed scientific journals, and his articles have been cited 3570 times. He is an expert in block copolymer synthesis and their application as an electrolyte for various fuel cells. His primary research interests include the development of novel electrocatalyst and electrolyte materials for proton-exchange membrane fuel cells, anion-exchange membrane fuel cells, water splitting, lithium-ion batteries, solar cells, and microbial fuel cells. His work also focuses on the development of potential sensors for the electrochemical detection of various biomolecules and the chemosensing of cancer cells. He has conducted many projects with the Korea Institute of Energy Technology Evaluation & Planning (KETEP) and the National Research Foundation (NRF).

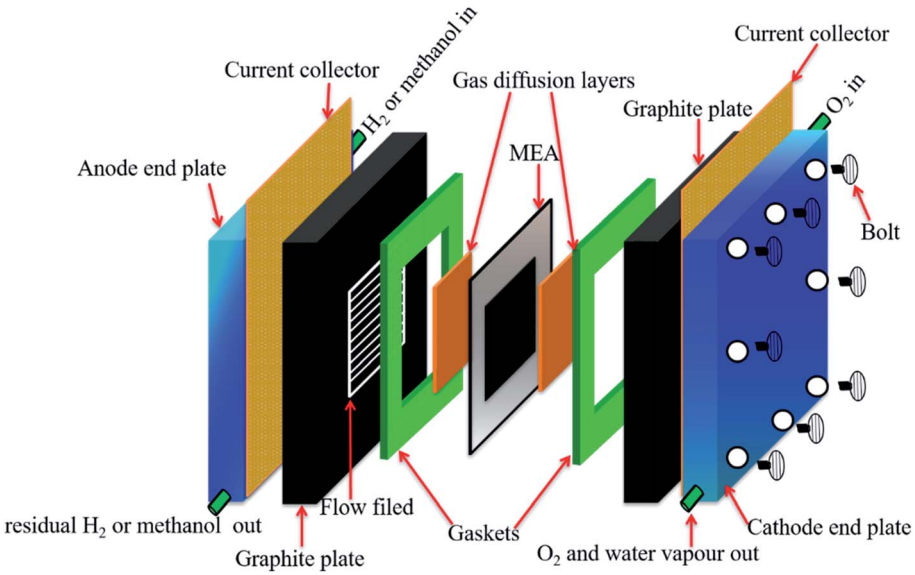

Fig. 2 Schematic representation of the working components of a single PEMFC.

two protons and two electrons, generating water and heat. The reaction of the cathode is as follows.[26]

$$\frac{1}{2}O_2 + 2H^+ + 2e^- \rightarrow H_2O \quad (2)$$

The overall reaction of PEMFC is thus as follows.

$$\frac{1}{2}O_2 + H_2 \rightarrow H_2O + \text{heat} + \text{electrical energy} \quad (3)$$

This review focuses on PEM, which performs as a conductor to transfer protons from the anode to the cathode and separator to preclude the contact of H_2 and O_2, because PEM underpins the overall efficiency of PEMFC. In addition to high proton conductivity and H_2/O_2 impermeability, the PEM should contain the following properties to give high PEMFC performance: (i) high electrical insulation, (ii) high mechanical integrity, meaning it is not deformed during applying the load, (iii) good hydrolytic, chemical, electrochemical, and thermal stabilities under fuel cell conditions, (iv) excellent water uptake to mitigate the cathode flooding issue in fuel cells, (v) low swelling degree during the long-term operation of the fuel cell, (vi) flexibility with different fuels, and (vii) good cost competitiveness.[3] Table 1 exhibits the various types of PEMs and their properties.[27,28]

Despite diverse types of PEMs having been developed, the state-of-the-art PEM for commercial PEMFCs is Dupont's Nafion as it can afford high proton conductivity at a low temperature and hydrated condition, low electronic crossover, and good chemical and mechanical stabilities.[29–34] These impressive characteristics of Nafion may be due to the combination of the hydrophobic polytetrafluoroethylene (PTFE) backbone and hydrophilic perfluorinated pendant side chains ending with sulfonic acid ($-SO_3H$) moieties (Fig. 3).[35–37] It could be assumed that the proton-conducting channels of Nafion can be generated between the $-SO_3H$ groups. Nevertheless, so far there is no experimental evidence of this to prove the creation of these ion channels in Nafion. The formation of ion channels and proton-transport properties can be explained only by several theoretical assumptions in the literature.[35,38] For instance, $-SO_3H$ groups in Nafion are assumed to be in the form of ionic clusters (~4–6 nm size) that are interconnected through narrow channels (~1 nm size).[35,38] Therefore, until now, Nafion has been used as the reference membrane for all PEMs used in PEMFCs.[39] The Nafion membrane has demonstrated a better proton conductivity of 0.130 S cm^{-1} at 75 °C and 100% relative humidity (RH) with a prolonged durability of about 6000 h under PEMFC operating conditions in relation with other PEMs.[40] At the same time Nafion has some significant drawbacks. It can be seen that the proton conductivity of Nafion membranes dramatically decreases under low RH and high temperature as it needs exterior humidification.[41] Besides, Nafion exhibits a high methanol crossover, which is mostly an unfavorable aspect for direct methanol fuel cells (DMFCs).[42] On the other hand, the Nafion membrane is also pricier ($711 for a 61 × 50 cm^2 Nafion-117 membrane), with the price currently soaring, which hinders the adoption of the Nafion membrane for large-scale applications.[3]

The aforementioned drawbacks of Nafion have encouraged researchers to propose various strategies to improve the performance of Nafion or to entirely replace Nafion in PEMFCs. Mostly, alternative PEMs have been developed based on aromatic hydrocarbon polymers, such as sulfonated poly(ether ether ketone),[43–46] sulfonated poly(ether imide),[47] sulfonated poly(-arylene ether sulfone),[48] and polybenzimidazole.[49] Most of the aforementioned PEMs were also developed as composite membranes with organic or inorganic fillers. Although most of the alternative PEMs were developed with a comparable/better PEMFC performance in relation to that of Nafion, their practical durability (under real-time fuel cell stack conditions) has

Table 1 Overview of the structure–property relationship of various PEMs used in PEMFCs[27,28]

PEM category	Structure	Advantages	Disadvantages
Perfluorinated membrane (Nafion)	(i) Polytetrafluoroethylene backbone	(i) Excellent proton conductivity at low temperature (<80 °C and hydrated condition)	(i) Proton conductivity decline at high temperature and low RH
	(ii) Perfluorinated pendent side chains ending with SO_3H groups	(ii) Good chemical and mechanical stability	(ii) High H_2/methanol crossover
			(iii) High cost
Partially fluorinated membranes	(i) Fluorocarbon backbone	(i) Low cost	(i) Low durability compared to perfluorinated membranes
	(ii) Hydrocarbon or aromatic side chain grafted onto the backbone	(ii) Low H_2 or methanol crossover	(ii) Low PEMFC performance, but performance can be tuned by suitable modification
		(iii) Backbones with good-anti free radical oxidation	
Fully hydrocarbon or non-fluorinated membranes	(i) Aromatic hydrocarbon backbones functionalized with polar or SO_3H groups	(i) More cost effective than perfluorinated membranes (ii) Proton conductivity can be tuned based on the degree of sulfonation (iii) High mechanical integrity	(i) Low durability compared to perfluorinated membranes (ii) High swelling degree
Acid–base hybrid membrane	(i) Integration of acidic component into the base polymer matrix or integration of base component into the acid polymer matrix	(i) Good chemical and thermal stability	(i) Poor durability under PEMFC operating conditions
		(ii) High proton conductivity compared to perfluorinated membranes	
Ionic liquid-based membranes	(i) Obtained by organic cation and an organic/inorganic anion, fluorocarbon backbone, hydrocarbon or aromatic side chain grafted onto the backbone	(i) High chemical, electrochemical and thermal stability	(i) Difficult to get a solid electrolyte membrane
		(ii) High proton conductivity under low RH (iii) Non-volatile	

still not been realized due to their poor PEMFC performance/durability ratio. Hence, Nafion still remains the standard PEM for PEMFC, and many efforts are currently underway to overcome the limitations of Nafion membranes, especially the fabrication of Nafion-based hybrid membranes. Until now, Nafion has been mixed with diversified materials: (i) aromatic and aliphatic polymers,[50,51] (iii) inorganic fillers,[52] (iv) ionic liquids,[53] and (v) carbon nanomaterials (CNs).[54] The use of aromatic or aliphatic polymers for composing with Nafion usually reduces the durability of Nafion, but effectually increases the proton conductivity of Nafion. In contrast, the use of inorganic fillers allows Nafion to afford an improved thermomechanical stability and durability but reduces the proton conductivity of Nafion. Hence, a better filler should be found to address Nafion's proton conductivity and durability. Recently, research on CNs has been progressing because the incorporation of CNs in the Nafion matrix allows achieving the maximum benefits of PEM. CNs, such as graphene oxide (GO),[54] graphene,[55] carbon nanotubes (CNT),[56] and fullerene,[57] have been widely explored as fillers in Nafion owing to their excellent mechanical, chemical, and thermal stability and fuel-blocking capability in PEM. As these CNs are electron conductors, the filler quantity incorporated into Nafion should be lower than 1 wt% in order to prevent electron crossover through PEM. For instance, one report states that the integration of CNTs with a weight ratio of 2–3 wt% in PEM leads to the excessive electron conductivity of PEM.[58] Nevertheless, it varies depending on the orientation and electrical conductivity of the host polymer matrix. Another key point is the absence of proton-conducting groups in CNs, since they dilute the density of $-SO_3H$ groups when incorporated into the Nafion matrix. It should be noted that CNs were previously usually functionalized by grafting on proton-conducting groups, such as $-SO_3H$,[55] phosphonic acid ($-PO_3H_3$),[59] amine ($-NH_2$),[46] and carboxylic acid ($-CO_2H$).[60] This approach allows increasing the density of ionic groups per unit volume of Nafion and thus facilitates the proton conductivity and PEMFC performance. On the other hand, functionalized CN (FCN) should be stable at high temperature, in a radical environment ($HO^{\bullet}$ and $HOO^{\bullet}$ radicals under fuel cells operating condition), and at various pH values, since it could help to avoid the proton-conductivity decline caused by the demolition of the

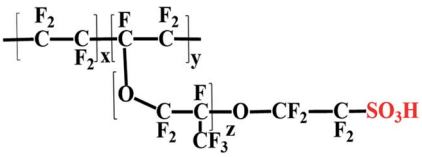

Fig. 3 Chemical structure of the Nafion membrane.

ionic channels. Recently, a few review articles aimed to collect together the significant efforts on CNs in PEMs, with a particular emphasis on GO. For instance, Rambabu *et al.* reviewed the application of CNTs, GO, and other carbon materials in DMFC membranes.[61] By contrast, Pandey *et al.* focused only on GO-based materials for fuel cell membrane applications.[62] Although, immense efforts have been put forward to collect the efforts on potential CN-based PEMs for PEMFCs, the mechanisms involved in the fabrication of FCNs, the importance of the incorporation of FCNs into the Nafion matrix, and the advantages of Nafion/FCNs membranes in PEMFCs and DMFCs, still need to be understood in order to promote their commercial adoption in real-time fuel cells. Hence, this review aimed to emphasize the mechanism involved in the proton conductivity of PEM, the essential requirements for PEMs, and the significant efforts done on the fabrication and implantation of Nafion/CN and Nafion/FCN membranes in PEMFCs and DMFCs.

2. Proton-transfer mechanism in PEMs

In general, proton transportation in the membrane occurs *via* two different mechanisms: the Grotthuss and vehicle mechanisms.[63,64] In the Grotthuss mechanism, protons transfer through the hydrogen-bond networks between the water molecules and ionic groups, in which the strength and length of the hydrogen bonds are highly important for successful proton transfer. Whereas, the vehicle mechanism involves the diffusion of protons along with the carrier ion ($H^+(H_2O)_n$) existing in the membrane and this mechanism is triggered by electro-osmatic drag and the concentration gradient of the aqueous medium. The activation energy (E_a) required for proton transfer with the Grotthuss mechanism is between the range of 9.65–38.59 kJ mol^{-1}, and for vehicle mechanism is about 16.4 kJ mol^{-1}. Under fully hydrated conditions, the protons are able to transfer through the carrier ions ($H^+(H_2O)_n$) in membranes.[20,65] Thus, the vehicle mechanical dominates in the PEM when operating the fuel cell under 100% RH. Under low RH or anhydrous conditions, the protons can only possibly diffuse through the hydrogen-bond networks due to the insufficient water molecules in the PEM. Thus, the Grotthuss mechanism mostly dominates when operating the fuel cell under low RH conditions.

3. Essential requirements for PEMs for PEMFCs

3.1. High thermal stability and glass transition state

In general, the operation of PEMFCs at high temperature (more than 100 °C) effectively boost their performance by enhancing the reaction kinetics of the electrode, limiting the requirement for excessive precious metal catalysts, also increasing the fuel diffusion rate and tolerance to fuel impurities.[66–68] Furthermore, PEMFC operation in the range of 100–150 °C is preferable from the point of view of heat and water managements because it does not require humidification, electro-osmatic drag, or a methanol reformer or hydrogen desorbing units.[68] Hence, the PEM should comprise a higher thermal stability and glass transition temperature (T_g) than the operating temperature of PEMFC. Mostly, Nafion demonstrated three stages of thermal degradation during the thermogravimetric analysis (TGA): (i) 280–400 °C, which may be due to the splitting up of –SO_3H groups, (ii) 400–470 °C, which may be due to the decomposition of the side chains, and (iii) 470–560 °C, which may be caused by degradation of the PTFE skeleton.[69–71] Meanwhile gases such as SO_2, H_2O, and CO_2 were liberated in the range of 25–355 °C, while gases such as COF_2, SiF_4, and HF were liberated at high temperature. When we consider the operating range of a PEMFC (100–150 °C), the H_2O and CO_2 gases mostly need to be taken into account. Apart from that, the T_g of Nafion can generally be observed at three regions during the first scan in differential scanning calorimetry (DSC): (i) 123 °C, which can be ascribed to the ionic cluster's phase transition, (ii) 183 °C, which is related to the hydrophobic segment's melting, and (iii) 213 °C, which is due to the rupture of ionic clusters.[72,73] Once the ionic clusters of Nafion have been ruptured, it is no longer feasible to retain the original cluster morphology of Nafion. Accordingly, most of the second DSC scan curves of Nafion adopt a flat shape. The incorporation of metal oxides, zeolites, and FCN in Nafion have been demonstrated to be one of the best strategies to improve the thermal stability and T_g of Nafion. Vinothkannan *et al.* incorporated Fe_3O_4-SGO, CeO_2-ACNT, and CeO_2-TiC into Nafion and concluded that the improved thermal stability and T_g of the composite membrane were associated with the interaction of the polymer and the fillers.[54,73,74]

3.2. Excellent mechanical and oxidative stability

The PEM employed in fuel cells is always placed between the bipolar plates, where it experiences severe mechanical stress, which leads to the cyclical swelling and shrinking of the PEM and consequently delamination of the PEM from the gas-diffusion layers. The mechanical stress can also exacerbate the internal defects (*i.e.*, formed during the preparation of the PEM or during the membrane electrode assembly) in the PEM. Altogether, these factors result in the generation of cracks, perforations, and tears in the PEM, thereby leading to failure of the PEMFC. Therefore, mechanically strong PEM with a high flexibility and low rigidity are mostly preferable for the long-term operation of the PEMFC.[75,76] As a matter of fact, the mechanical integrity of the PEM is influenced by various factors, such as the thickness of the PEM, type and wt% of the filler, electrostatic interactions between the polymer and the filler, type of polymer backbone in the PEM, and degree of sulfonation of the PEM.[77] For instance, the strong hydrogen bonding between the C–F (from the PTFE backbone) and –SO_3H groups (from the pendent side chains) of Nafion leads to close chain packing; thereby increasing the mechanical strength of the Nafion membrane. The mechanical strength of Nafion can be further improved by making the composite with FCNs. For example, Sahu *et al.* reported that 1 wt% sulfonated graphene (S-graphene) loading can enhance the mechanical integrity by a few fold.[55] This result is due to the effectual load transfer of Nafion to the S-graphene through the hydrogen bonds. However, the incorporation of a high quantity of S-graphene

(more than 1 wt%) into Nafion leads to aggregation, which may enhance the brittleness of PEM and reduce its mechanical integrity. Therefore, strategies must find a way to prepare the PEM with an optimized filler content, which would not only improve the mechanical stability but also the physicochemical and electrochemical properties. Dynamic mechanical analyzers (DMAs) and universal test machines (UTMs) have been extensively used to quantify the mechanical integrity of PEMs.[78,79] The storage modulus, loss modulus, and tan δ of PEMs can be measured by DMA, whereas the UTM can help quantify the tensile strength, elongation at break, and Young's modulus of the PEM.

The entire active surface of the PEM is always exposed to intermediates (H_2O_2) and free radicals ($HO^{\bullet}$ and $HOO^{\bullet}$) that are formed during the sluggish two-electron reduction of O_2 on the cathode.[80,81] These radicals attack the functional groups (–CO_2H, –SO_3H, and R–O–R are more vulnerable to radicals) in the PEM and unzip the polymer chains, which results in thinning of the bulk polymer, as well as the production of local defects in the PEM.[82,83] Besides, the radical attack further exacerbates the defects formed by mechanical stress. Altogether, these harmful factors lead to increased fuel permeability through the PEM and suppress the PEMFC performance and durability. Chemical degradation of the PEM in PEMFCs can be aggravated by factors such as the cell temperature and RH, back pressure, external load, and fuel concentration. This is the rationale behind the evaluation oxidative stability of the PEM prior to PEMFC operation. Fenton's test is commonly used to quantify the *ex situ* durability of a PEM, in which changes occur in the weight of the PEM upon exposure to Fenton's reagent (3% PPM $FeSO_4$ in 5% H_2O_2) at 80 °C have measured. During the test, Fenton's solution continuously generates radicals as per the following.[80]

$$H_2O_2 + H^+ + Fe^{2+} \rightarrow HO^{\bullet} + H_2O + Fe^{3+} \quad (4)$$

$$H_2O_2 + Fe^{2+} + Fe^{3+} \rightarrow HOO^{\bullet} + H^+ \quad (5)$$

In general, Nafion and its composites exhibit excellent oxidative stability, leading to prolonged fuel cell operation with sustainable power performance, which can be ascribed to its PTFE backbones. The oxidative degradation of Nafion can be further mitigated by incorporating radical-scavenging materials (*e.g.*, CeO_2,[80,84] ZrO_2,[85] ferrocyanide-coordinated polymer,[86] and $Zr_2Gd_2O_7$ (ref. 31)). However, applying these fillers to the Nafion matrix, which does not have proton-conducting groups, can cause a proton conductivity decline in the PEM. Besides, the lower interaction of the aforementioned fillers with the Nafion matrix can lead to removal of the fillers from the PEM, and thus, an ineffective radical-scavenging activity. Introducing templates to stabilize the radical scavengers in the PEM would be the best solution to avoid the leaching of the fillers. Vinothkannan *et al.* exploited amine-functionalized CNT to stabilize CeO_2 in the Nafion matrix. They also achieved a simultaneous improvement in the proton conductivity and oxidative stability for a Nafion/CeO_2-ACNT membrane compared to pristine Nafion and Nafion/CeO_2 membranes.[73]

3.3. Excellent water-uptake capacity and dimensional stability

Since the water-uptake capacity of PEMs is inevitable for the facile transfer of protons from the anode to the cathode and to avoid the cathode flooding issue, the water-uptake capacity of a PEM influences the performance of PEMFCs. In general, the water-uptake capacity of a PEM is affected by various parameters, such as cell temperature and RH, density of the ionic groups, type of filler materials, and elasticity of the polymer matrix. The detailed and most common protocol to quantify the water uptake of PEMs can be found in the literature.[87,88] The time and temperature applied for water-uptake measurement can vary case by case. Mostly, the water-uptake capacity of the Nafion membrane is slightly lower compared to other hydrocarbon membranes due to its hydrophobic PTFE backbone. It has been reported that the incorporation of FCN-based fillers could effectively improve the water uptake of PEMs rather than other inorganic fillers.[43] Nevertheless, excessive water uptake causes a problem to the PEM as it creates excessive swelling in the length and thickness direction of the PEM. If FCN is incorporated into the PEM, the degree of swelling in the length direction decreases because FCN-based fillers are mostly dispersed in the in-plane direction of the PEM. For example, the literature reports that 2 wt% of sulfonated CNT or sulfonated GO in PEM is the percolation threshold leading to reduced swelling in length direction.[89] However, PEM swelling in the thickness direction increases with the increasing water uptake. The increased swelling of PEM in the thickness direction is mostly compensated by the compression of a membrane electrode assembly (MEA) when fixed in a PEMFC device. Hence, FCN-based fillers can be employed to achieve a higher water uptake with a low reduced swelling degree of PEMs. The most common equations to obtain the water uptake and swelling degree of PEMs are as follows.

$$\text{Water uptake } (\%) = \left[\frac{\text{weight of wet PEM} - \text{weight of dry PEM}}{\text{weight of dry PEM}}\right] \times 100 \quad (6)$$

$$\text{Swelling degree } (\%) = \left[\frac{(\text{length of wet PEM} \times \text{thickness of wet PEM}) - (\text{length of dry PEM} \times \text{thickness of dry PEM})}{(\text{length of dry PEM} \times \text{thickness of dry PEM})}\right] \times 100 \quad (7)$$

3.4. Ion-exchange capacity and hydration

The ion-exchange capacity (IEC) of PEMs, which demonstrates the quantity of ionizable groups in a PEM, is believed to be usually well correlated with the proton conductivity.[55,90] Measurements of the IEC are normally conducted with the acid–base titration method. In most Nafion membranes incorporated with FCNs or inorganic fillers, the IEC increases as the loading quantity of the filler increases. Parthiban *et al.* found that the IEC of Nafion always increased when the loading of S-graphene increased for Nafion/S-graphene membranes.[91,92] Detailed protocols to quantify the IEC can be seen in the literature and the following equation is mostly used to calculate the IEC of a PEM.[93–95]

$$\mathrm{IEC}\ \left(\mathrm{meq\ g^{-1}}\right) = \frac{\text{volume of NaOH consumed} \times \text{concentration of NaOH}}{\text{weight of dry sample}} \quad (8)$$

The hydration number of a PEM can be defined as the number of bound water molecules attached per unit volume of $-SO_3H$ groups in the PEM.[96,97] The hydration number of a PEM is the ratio of the water uptake and the IEC. The hydration number calculation also gives information on the bound water-retention capability of a PEM. Generally, the hydration number of a PEM can be calculated with the equation given below, where the 18.01 is the molecular weight of water.[98]

$$\text{Hydration number} = \left[\frac{\text{water uptake}}{18.01}\right]\left[\frac{10}{\mathrm{IEC}}\right] \quad (9)$$

3.5. Self-humidification capability

The water content of a PEM must be maintained throughout the PEMFC operation and it should not be removed even at high temperature or low RH. However, the water molecules in the PEM are frequently removed at high temperature or low RH, which leads to the dehumidification of PEM and suppressed PEMFC performance. The incorporation of hydrophilic domains through inorganic materials[30,99,100] (heteropolyacids, Fe_3O_4, SiO_2, CeO_2, ZrO_2, and TiO_2) into the PEM matrix enhances the binding capacity of water with the PEM. Water molecules can easily attach to the hydrophilic domains of inorganic materials through hydrogen bonding, and in that way, water can be retained in the PEM effectively, even at high temperature or low RH. However, the incorporation of hygroscopic–inorganic fillers would reduce the density of $-SO_3H$ groups per unit volume of the PEM matrix, and hence, the proton conductivity of the PEM may reduce under fully hydrated conditions. On the other hand, many reports have demonstrated that the incorporation of $-NH_2$-functionalized CN into the PEM can facilitate the PEMFC performance both under hydrated and low RH conditions.[46,73,101] Therefore, the FCN-based PEM can be considered as an optimized PEM for both hydrated and low RH fuel cells.

3.6. Proton conductivity

The generated protons at the anode during fuel oxidation should effectively transfer to the cathode *via* the PEM to continue the viable fuel cell operation. The good proton-transport properties of a PEM can effectually reduce the ohmic and mass-transport losses of the cell, and hence outstanding power and current outputs of a PEMFC can be obtained. Usually, the PEM conducts the protons *via* its viable conducting channels constructed by the acidic or basic functionalities ($-SO_3H$, $-PO_3H_3$, $-NH_2$ $-OH$, and $-CO_2H$) that exist in the PEM itself. The proton conductivity of a PEM can be influenced by diverse factors, such as the temperature, RH, water-retention capability, ionic cluster size in the PEM, density of proton-transfer channels (acidic or basic functionalities), tortuosity, and chemical interaction between the filler and polymer. Among these factors, the interaction between the polymer and filler is more significant, which effectually reduces the E_a for proton travelling by facilitating rapid proton hopping. In addition, these proton-transfer channels firmly improve the water-retention ability, which prevents the PEM from dehydration during low RH operation. Mostly, the proton conductivity of a PEM is evaluated by four-point alternating-current impedance spectroscopy.[102,103] There are two types of measurements to quantify the proton conductivity of a PEM: (i) in-plane and (ii) through-plane. In the case of in-plane measurements, the proton transport can be determined within the plane of the membrane. For the through-plane measurement, the proton transport can be determined through the thickness of the membrane. Although through-plane measurements are more relevant for PEMFCs, the in-plane measurement is easily implemented and thus often reported.[54,55] The proton conductivity (σ, Siemens per centimeter (S $\mathrm{cm^{-1}}$)) of a PEM can be acquired using the equation given below.[102,103]

$$\sigma\ \left(\mathrm{mS\ cm^{-1}}\right) = \frac{L}{RTW} \quad (10)$$

where L is the distance between the electrodes in the cell (fixed, but based on the conductivity cell used), T (cm), W (cm), and R (Ω) denote the PEM's length, thickness, width, and ohmic resistance, respectively.

3.7. Electronic insulation

Since PEMs incorporated with CN-based fillers conduct electrons when applied in a PEMFC, this could lead to various disorders, such as internal short circuiting, voltage drop, and chemical degradation of the PEM. Therefore, the electrical conductivity of CN-based fillers has to be reduced to facilitate the PEMFC performance. The covalent grafting of functional groups or the doping of metal oxides on the surface of CNs have been demonstrated to be potential routes to reduce the electrical conductivity of CNs.[54,55] The electrical conductivity of a PEM can be measured by an electrometer conjugated with four Pt probes. The following equation has been frequently exploited to calculate the electrical conductivity (σ) of a PEM.[60]

$$\sigma\ \left(\Omega^{-1}\ \mathrm{cm^{-1}}\right) = \frac{G \times l}{A} \quad (11)$$

where G is the conductance of the PEM in Siemens, l is the thickness of the PEM in cm, and A is the active surface area of the PEM in $\mathrm{cm^2}$.

3.8. Fuel crossover

In general, fuel crossover (H_2 or methanol) through the PEM is considered a key drawback that diminishes the overall performance of fuel cells by reducing the fuel efficiency, hindering the electrochemical reaction at the electrode membrane interface, decreasing the proton transport, and accelerating the HO$^{\bullet}$ and HOO$^{\bullet}$ radical formation.[31,80,84] Fuel crossover mainly occurs due to the formation of pinholes, tears, and cracks in the PEM as a result of the chemical, mechanical, or thermal degradation of PEM.[89] The low fuel crossover of the PEM is extremely essential to attain the low fuel consumption and enhanced power density and durability of the fuel cell. Several strategies, such as the incorporation of 2D sheets in the PEM, fabrication of a thicker PEM, blending of hydrophobic materials with the PEM, and operating the cell at a low current density, have frequently been used to decrease the fuel crossover effectively.[42,104,105] On the other hand, the utilization of Pt- or Pt–Ru-based fillers in the PEM would help to oxidize the H_2 or methanol within the PEM while passing through it, thereby precluding fuel crossover. However, the aforementioned strategies may cause several limitations, including a decrement in proton conductivity and activation and ohmic losses, which again would reduce the power density of fuel cells. Nevertheless, the incorporation of FCNs has been demonstrated as one of the best strategies to precluding the fuel crossover by generating tortuous paths through the PEM and for improving the proton conductivity by increasing the density of ionic groups in the PEMs.[92–94] Hence, FCN fillers must be developed and incorporated into the PEM to achieve competent electrolyte materials for fuel cells. From the literature, most researchers have quantified the fuel crossover through the PEM by linear sweep voltammetry (LSV) using the potentiostat/galvanostat, and the detailed protocols to quantify the fuel crossover of PEM can be found in the literature.[92–94] Determining the limiting current density related to the plateau region is considered one way to calculate the fuel crossover of a PEM. The crossover flux of fuel can be evaluated by the following equation.[106]

$$J_{\text{flux}} = \frac{i_{\text{lim}}}{(nF)} \quad (12)$$

where i_{lim} is the limiting current derived from the LSV, n is number of electrons involved in the reaction, and F is Faraday's constant.

3.9. Good compatibility with the Pt/C catalyst during the fabrication of the membrane electrode assembly

Another important requirement to attain high PEMFC performance and durability is the compatibility of the PEM with the Pt/C catalyst. There seem to be three types of membrane electrode assemblies (MEAs) that have been mostly preferred for PEMFCs by most researchers (Fig. 4):[31,107,108] (i) catalyst-coated membrane (CCM), (ii) catalyst-coated gas-diffusion layer (CCG), and (iii) catalyst-coated substrate (CCS). For fabrication of the CCM, Pt/C slurry (Pt/C + deionized water + Nafion resin + isopropyl alcohol) is coated on the PEM directly by an air-spraying or brushing method. In the case of CCG, the Pt/C slurry is coated on a gas-diffusion layer (GDL) by an air-spaying, brushing, or printing method. Then, the Pt/C-coated GDL is switched for both sides of the PEM. For the CCS, the Pt/C slurry is initially coated on the two substrates and then the substrates are coupled to both sides of the PEM. After the Pt/C is attached on PEM, the substrate is directly detached from the PEM using forceps. One of the simple strategies to improve the compatibility of the PEM with the Pt/C catalyst is to make the PEM with a rough surface, which increasing the adhesion of the catalyst on the PEM and reduces the total MEA resistance. Parthiban *et al.* increased the surface roughness of the PEM by incorporating S-graphene, and thus, the adhesion of the Pt/C catalyst was increased and the resistance of the MEA was decreased when applied in a PEMFC.

4. CN- and FCN-based additives for Nafion applicable for fuel cells

Significant efforts have been made on CN- and FCN-based additives for Nafion applicable for fuel cells during the last decade. This section covers the preparation strategies and significant achievements of PEMs in fuel cells.

4.1. CNT and functionalized-CNT (FCNT) for PEMs

CNTs are a one-dimensional tubular-like material made by sp^2 hybridized carbon atoms, and have attracted much attention as a reinforcing material for polymers, due to their remarkable tensile strength (about 63 GPa, which is 50-fold higher than steel) and stiffness, low density, high aspect ratio, and optical properties.[61,73,109] Generally, CNTs can be categorized as single-walled CNTs (SWCNTs) and multi-walled CNTs (MWCNTs) and both have been widely exploited as fillers for PEM applications.[110–112] However, MWCNTs are a preferred choice over SWCNTs owing to their lower electrical conductivity and more surface defects, which are important for use in PEMs.[113] Mainly, CNTs are chosen as an additive to address the fuel permeability and mechanical integrity issues of Nafion in PEMFCs. Nevertheless, the uniform dispersion of CNTs is difficult owing to the van der Waals interactions between the individual tubes, which limits the interfacial interaction with the polymer matrix. To overcome this issue, the surface modification of CNT is frequently performed with diversified functionalities or metal oxides, including –SO_3H–, –P_2O_5, CO_2H, –NH_2, Fe_3O_4, SiO_2, and CeO_2.[58,60,73,114–116] The research efforts done on CNT- and FCNT-based Nafion composite membranes applicable for PEMFC and DMFC are discussed below.

4.1.1. Nafion/CNT or FCNT composite membranes for PEMFCs. Chen *et al.*[117] developed polysiloxane-functionalized CNT (CNT-EO) by the covalent grafting of poly(oxyalkylene) diamines and tetraethyl orthosilicate-reinforced polysiloxane in a layer-by-layer manner. This was followed by the CNT-EO being blended with Nafion *via* a solution-casting technique, and then the effects of the CNT-EO content on the proton conductivity of the composite membrane were analyzed. The maximum proton conductivity exhibited by CNT-EO/Nafion containing 20 wt% CNT-EO was 0.093 S cm^{-1}, which was higher than that of 5, 10,

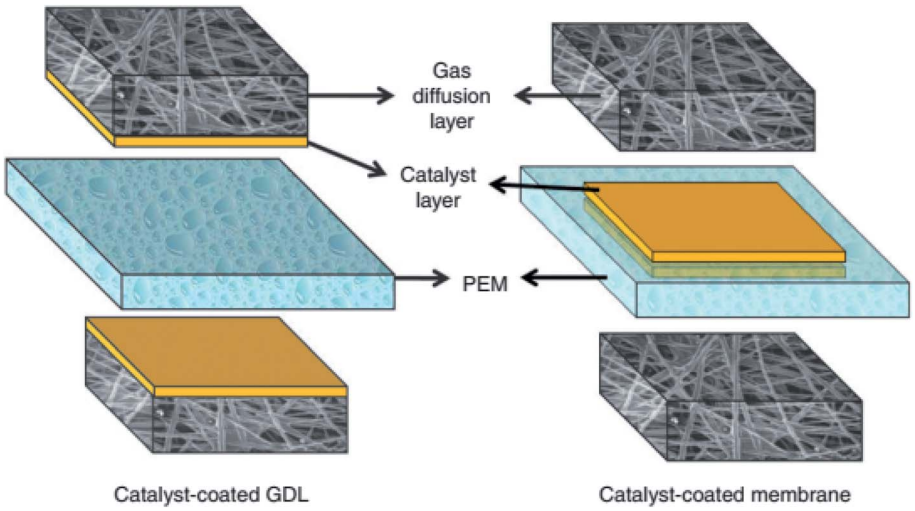

Fig. 4 Schematic representation for CCG and CCM. Reused from ref. 107 with permission from Elsevier, 2009.

or 15 wt% CNT-EO/Nafion membranes, suggesting that an optimized filler content in the membrane is extremely essential for enhanced proton conductivity. Kannan *et al.*[118] sulfonated SWCNTs and subsequently incorporated these into Nafion (S-SWCNT/Nafion) through a solvent-casting approach and the prepared PEM was then employed as an electrolyte in a PEMFC. The excess of $-SO_3H$ moieties anchored on the surface of S-SWCNT could provide more facile paths for the hopping of protons, which promoted the proton conductivity of the composite PEM to a higher extent. Thereby, the S-SWCNT/Nafion could achieve a power output of 260 mW cm^{-2} when operating the PEMFC at 60 °C under 100% RH. By comparison, Nafion 1135 was only able to achieve 210 mW cm^{-2} under identical operating conditions. The same group also tuned the proton conductivity of Nafion by manipulating the hydrophilic domains of Nafion by integrating S-MWCNTs.[119] Consequently, the Nafion composite PEM with 0.05% S-MWCNTs demonstrated a PEMFC power density of 380 mW cm^{-2}, which was better than that of Nafion 115 (250 mW cm^{-2}) and bare Nafion (230 mW cm^{-2}) PEMs. A CNT-reinforced Nafion composite PEM was prepared by Liu *et al.* for a H_2/O_2 fuel cell.[120] The incorporation of 1 wt% CNT in the Nafion PEM could enhance its mechanical strength and dimensional stability, while retaining the performance of the H_2/O_2 fuel cell. Ijeri *et al.*[121] investigated the effect of CNT (0–5 wt%) on the proton and electron conductivities of Nafion. The electrical conductivity of a Nafion/CNT membrane was found to be increased with increasing the wt% of CNTs in the Nafion matrix, owing to the electron-conducting nature of the CNTs. On the other hand, the proton conductivity of the Nafion/CNT membrane decreased with increasing the CNT content. However, the wet Nafion/CNT membrane showed higher proton conductivity compared to the dry membrane. CNT, oxidized CNT (oCNT), and amine-functionalized CNT (fCNT) were incorporated into Nafion individually by Cele *et al.*[122] The thermal stability, thermo-mechanical stability, and proton conductivity of the Nafion/CNT, Nafion/oCNT and Nafion/fCNT were quantified and compared. The Nafion/oCNT PEM showed a concurrent increment in most of the properties compared to the other PEMs. This may be attributed to the better interaction of $-CO_2H$ groups of oCNT with $-SO_3H$ groups of Nafion. Liu *et al.*[123] developed Nafion-functionalized MWCNT (Nafion-MWCNT) *via* an ozone-mediated process. They blended 0.025, 0.05, 0.1, and 0.2 wt% Nafion-MWCNT with Nafion to obtain Nafion-MWCNT/Nafion hybrid PEM. Among these, the hybrid membrane with 0.05 wt% filler achieved the best proton conductivity. Thus, in the fuel cell test, the hybrid membrane with 0.05 wt% filler delivered a peak power output and current output at 0.6 V of 650 mW cm^{-2} and 1556 mA cm^{-2}, respectively. Both values were 1.5-fold higher than those of bare Nafion. Tortello *et al.*[124] vertically aligned CNTs in the Nafion matrix at a weight ratio of 7 wt% by applying an electric field. They quantified the electron and proton conductivity of Nafion/CNT (7 wt%) under both ambient and wet conditions. The proton conductivity of the PEM was more significantly improved under wet condition than under ambient condition. Steffy *et al.*[125] investigated a Nafion/SMWCNT hybrid membrane for a perspective PEMFC under a low RH. The $-SO_3H$ networks present along the sidewalls of the SMWCNTs favored prompt proton transfer *via* the membrane, Therefore, the composite membrane rendered an enhanced power density of 549 mW cm^{-2} at a load current density of 1700 mA cm^{-2}, which was 8.1 fold higher than that of pristine Nafion (67 mW cm^{-2} at a load current density of 200 mA cm^{-2}). Yin *et al.*[126] laterally aligned the sulfonated CNT (Su-CNT) in the Nafion matrix through a layer-by-layer assembly. The prepared Nafion/Su-CNT membrane consisted of a certain number of equally thick Nafion and SCNT layers (1, 10, 20, 35, 50, and 80 layers). The satisfactory proton conductivity of the Nafion/Su-CNT (80 layer) membrane was retained even after 100 h of operation. Furthermore, owing to the layer-by-layer alignment of SCNTs, the tensile strength of Nafion/Su-CNT increased to ~40 MPa in the lateral direction. These results indicated that a multilayered structure of Nafion/Su-CNT could simultaneously promote the proton conductivity and

mechanical strength of membranes. He *et al.*[127] studied the effect of different functional groups (–PO_3H_2, –CO_2H, and –SO_3H) in CNTs on the proton conductivity of the Nafion membrane. A hybrid membrane containing 5 wt% phosphorylated CNTs (PCNTs) delivered the maximum proton conductivity, which was ascribed to the low-energy-barrier proton-conducting channels given by the PCNTs. Simari *et al.*[128] synthesized a new type of CNTs from smectite clays (SWy) using a chemical vapor deposition method, and functionalization of the CNTs was performed by an –SO_3H-containing organic moiety. The introduction of SWy-oxCNTs-RSO_3H enhanced the proton conductivity of Nafion to 0.070 S cm^{-1}, which was 1 order of magnitude higher than the plain Nafion membrane. Vinothkannan *et al.*[73] fabricated a potential bifunctional filler of a CeO_2-anchored amine-functionalized CNT (CeO_2-ACNT) for the Nafion matrix to enhance the electrochemical power density and durability of a PEMFC operating under both 100 and 20% RH (Fig. 5). The Nafion/CeO_2-ACNT composite membrane demonstrated a low/comparable power density of 270 mW cm^{-2} with recast Nafion (283 mW cm^{-2}) and Nafion-212 (261 mW cm^{-2}) under 100% RH. The main reason for the low power density of Nafion/CeO_2-ACNT membranes is due to the decrement of the density of –SO_3H groups in the Nafion matrix after the incorporation of CeO_2-ACNT. However, the acid–base interactions between the CeO_2-ACNT and Nafion promoted the power density of a PEMFC under 20% RH. Hence, the Nafion/CeO_2-ACNT membranes displayed a peak power density of 174 mW cm^{-2}, whereas the bare Nafion and Nafion-212 yielded only 83 and 72 mW cm^{-2}, respectively. Besides, the Nafion/CeO_2-ACNT membrane retained high durability with a low voltage decay both under 100 and 20% RH. This was due to the radical-scavenging activity of the CeO_2-ACNT.

4.1.2. Nafion/CNT or FCNT composite membranes for DMFCs. The activity of hydroxyl-functionalized MWCNTs (MWCNT-OH), sulfonated MWCNTs (MWCNT-SO_3H), and imidazole-modified MWCNTs (MWCNT-Im) were evaluated by incorporating them in the Nafion matrix by Tohidian *et al.*[129] Nafion/MWCNT-Im exhibited a lower methanol crossover and higher proton conductivity compared to the Nafion/MWCNT-OH and Nafion/MWCNT-SO_3H membranes. The obtained results were ascribed to the existence of acid–base proton-conducting pathways in the Nafion/MWCNT-Im membrane. Thomassin *et al.*[130] fabricated a MWCNT-COOH/Nafion composite membrane by engrafting MWCNT-COOH into the Nafion matrix with the aid of melt-extrusion. The mechanical, methanol barrier, and proton-conduction properties of the MWCNT-COOH/Nafion were effectually investigated. The methanol permeability of MWCNT-COOH, as evaluated from two-compartment cell measurements, was much lower than that of bare Nafion. Also, the observed proton conductivity and Young's modulus of MWCNT-COOH/Nafion was a few-fold higher that of bare Nafion. These unique properties were attributed to the definite pore size and excess acidic functional groups present in the composite membrane, suggesting that MWCNT-COOH/Nafion can be a pertinent electrolyte for DMFCs. Asgari *et al.*[131] functionalized histidine on CNTs through an imidazole group (Im-CNT). Afterward, the 0.5% Im-CNT was embedded into the Nafion matrix to realize a Nafion/

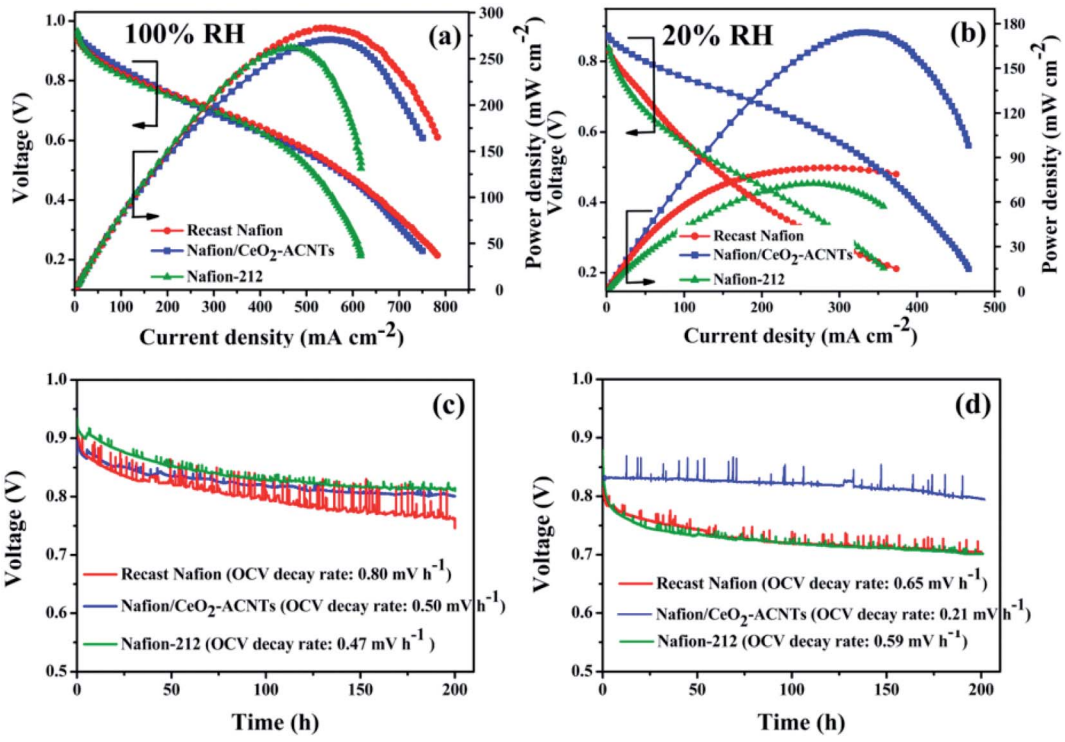

Fig. 5 PEMFC performance and durability of plain Nafion, Nafion/CeO_2-ACNT, and Nafion 212 membranes: (a, c) at 60 °C and 100% RH and (b, d) at 60 °C and 20% RH. Reproduced from ref. 73 with permission from the American Chemical Society, 2019.

Im-CNT-0.5% hybrid PEM for a DMFC. The DMFC power density of Nafion/Im-CNT-0.5% reached 61 mW cm^{-2} at 0.5 V when using 5 M methanol as the fuel, which was 1.4-fold high than that of bare Nafion (42 mW cm^{-2}). The obtained high power density was ascribed to the improved proton conductivity as well as the methanol barrier properties of Im-CNT. Fe_3O_4-anchored Nafion-functionalized MWCNTs (MWCNT-MNP-Nafion) were prepared and incorporated into the Nafion matrix by Chang *et al.*[132] The obtained MWCNT-MNP-Nafion/Nafion was highly effective in improving the DMFC power density from 12.5 mW cm^{-2} for bare Nafion to 92.4 mW cm^{-2} for the composite PEM. A further enhancement in DMFC power density was obtained by magnetically aligning the MWCNT-MNP-Nafion in the Nafion matrix. After aligning the filler, the DMFC power density of MWCNT-MNP-Nafion/Nafion was increased to 109.3 mW cm^{-2}, which was 8.7 times higher than the bare Nafion. Hasani-Sadrabadi *et al.*[133] exploited the Nafion/chitosan-wrapped CNT (CS-CNT) as an electrolyte in a DMFC. The Nafion/CS-CNT membrane was prepared by a direct blending of CS-CNT with a solution of Nafion and subsequent casting at 70 °C. The proton conductivity was increased by the formation of 1D long range ionic channels in the Nafion matrix, while the methanol permeability was suppressed through the interfacial interactions between the polymer and filler. Consequently, the Nafion/CS-CNT PEM brought about a single-cell power density of 110 mW cm^{-2}, which was a power density more than two times that of pristine Nafion 117 (47 mW cm^{-2}). Molla-Abbasi *et al.*[134] utilized a CNT@SiO_2-PWA/Nafion hybrid PEM as an electrolyte in a DMFC. This was synthesized *via* a solution-casting method, in which a CNT@SiO_2-PWA composite filler was directly mixed into a solution of Nafion, followed by casting at 70 °C. The methanol permeability value of the CNT@SiO_2-PWA/Nafion membrane was found to be 2.63×10^{-7} cm^2 s^{-1}, which was much lower than that of pristine Nafion (2.25×10^{-6} cm^2 s^{-1}). Also, the proton conductivity exhibited by the composite membrane was a few-fold larger than that of pristine Nafion. The aforementioned distinctive properties demonstrated that the CNT@SiO_2-PWA/Nafion membrane yielded a high selectivity toward protons rather than methanol, owing to the existence of CNT@SiO_2-PWA.

4.2. GO and functionalized GO (FGO) for PEMs

GO is a 2D sheet-like material (1.1 ± 0.2 nm thick), composed of combinations of sp^2 and sp^3 bonded carbon atoms, which bears hydrophilic-oxygenated functionalities (–OH, –O–, and –CO_2H) on its basal and edge planes.[44] The unique properties of GO, including larger specific surface area, open structure, functional groups, high Young's modulus, thin structure, and intrinsic mechanical and thermal stability, facilitate its use as a potential filler for PEMs. In addition, the exclusive amphiphilic nature (both hydrophilic and hydrophobic) of GO helps to simultaneously enhance the proton-transport and fuel-barrier properties of PEMs (mostly for DMFCs).[43] The hydrophilic functional groups (–OH, –O–, and –CO_2H) of GO have been reported to offer a proton conductivity of 0.001 S cm^{-1} at 300 K.[44] Besides, these functional groups enable GO to undergo further modification by chemical reaction for the introduction of various functional groups. Thus, both GO and FGO are used as potential fillers for PEMs.

4.2.1. Nafion/GO or FGO composite membranes for PEMFCs. An FGO/Nafion nanocomposite membrane was fabricated through a solution-casting method and employed as an electrolyte in a PEMFC at 120 °C under 25% RH by Zarrin *et al.*[66] When compared to GO/Nafion, the ionic conductivity of the F-GO/Nafion membrane was found to be three orders of magnitude higher at 20 °C and more than one order of magnitude higher at 80 °C, owing to the presence of excess ion-conduction channels in FGO/Nafion. Therefore, the maximum power output obtained for the FGO/Nafion (150 mW cm^{-2}) membrane was about 3.6 fold better than that of the recast Nafion (42 mW cm^{-2}). Besides, at a cell voltage of 0.6 V, the FGO/Nafion showed a current density of 160 mA cm^{-2}, which was about 3.5 times higher than that of the recast Nafion (46 mA cm^{-2}). Enotiadis *et al.*[135] functionalized GO with various functional groups (–NH_2, –OH, and –SO_3H) and embedded it into the Nafion matrix to realize a composite membrane. The Nafion-containing –SO_3H-functionalized GO provided for a high water uptake, and good proton conductivity and thermomechanical stability compared to other composite membranes, owing to the good dispersibility of the filler in the polymer matrix. Kumar *et al.*[136] exploited the Nafion composite membrane with 2, 4, and 6 wt% GO and applied these samples as the electrolyte in a PEMFC at 100 °C under 25% RH. Among the prepared membranes, the Nafion/GO (4 wt%) exhibited the highest proton conductivity of 0.044 S cm^{-1} at 120 °C, which indicated that 4 wt% GO would be an optimal loading for Nafion during high-temperature operation. The high proton conductivity of the Nafion/GO (4 wt%) membrane was attributed to a Grotthuss-type proton conduction *via* the hydrogen bond between the GO and Nafion. By this unique property, the Nafion/GO (4 wt%) membrane exhibited the maximum power density of 212 mW cm^{-2}, which was a few times higher than that of the recast Nafion and Nafion 212 membranes. Also, the Nafion/GO (4 wt%) membrane exhibited a current density of 440 mA cm^{-2} at a cell voltage of 0.47 V, (272 mW cm^{-2}), about 3.2 fold better than that of the Nafion-212 membrane. Aragaw *et al.*[137] investigated the impact of reduced GO (RGO) incorporation on both proton conductivity and electron conductivity of a Nafion/RGO composite membrane. The proton conductivity and electron conductivity of the Nafion/RGO composite membrane were found to be increased by 30 and 5 times, respectively, compared to the recast Nafion. The higher electron conductivity was due to the rapid electron delocalization through the RGO sheets, while the higher proton conductivity was due to the alignment of the proton-conducting channels in the Nafion/RGO membrane by the hot-press thermal reduction. Lee *et al.*[138] developed Pt-graphene (Pt-G) *via* a microwave deposition method. The Pt-G was then impregnated into Nafion to obtain a Nafion/Pt-G membrane, which was then used for a low humidity fuel cell. Due to the hydrophobic nature of the graphene and Pt nanoparticles, the Nafion/Pt-G membrane exhibited lower proton conductivity and water-uptake properties. Hence, the peak power density generated by the Nafion/Pt-

G membrane was lower than that of the Nafion/GO composite. However, the constant OCV of the Nafion/Pt-G even under low RH suggested that Pt-G could be used as a perspective filler for Nafion in the domain of low humidity PEMFCs. The same group also developed a Nafion/Pt-G/SiO_2 composite membrane with various weight ratios of Pt-G and SiO_2. Below 1.5 wt% Pt-G the PEMFC performance of the composite membrane increased with the SiO_2 content due to the water-retention properties of SiO_2. However, the performance decreased when the Pt-G content exceeded more than 1.5 wt% as a result of the proton-blocking effect of Pt-G.[139] Mishra *et al.*[140] fabricated Nafion/sulfonated poly(ether ether ketone)/highly oxidized GO (Nafion/SPEEK/HGO) nanocomposite membranes through a solution-casting method. It was employed as an electrolyte in a PEMFC and its effect on the degree of oxidation of GO in Nafion/SPEEK/GO was analyzed with respect to the fuel cell performance. The maximum power density noted with the Nafion/SPEEK/HGO was 621 mW cm^{-2}, which was about 97 mW cm^{-2} higher than the virgin Nafion membrane (524 mW cm^{-2}), indicating that the concentration of oxygen functionalities in GO predominantly influenced the proton-conduction properties of the composite membrane. Kim *et al.*[141] prepared a phosphotungstic acid-coupled graphene oxide (PW-mGO) and embedded this into a Nafion membrane (Nafion/PW-mGO). Owing to the high water retention capacity, reduced ohmic resistance, well-connected proton-transport channels, and strong hydrogen-bonding interaction, the Nafion/PW-mGO membrane exhibited a higher PEMFC power density of 841 mW cm^{-2} at 80 °C under 20% RH compared to bare Nafion (210 mW cm^{-2}). Sahu *et al.*[55] also introduced S-graphene into Nafion. They reported that the surface roughness of the Nafion membrane increased after the incorporation of S-graphene (Fig. 6), which facilitated the compatibility of the Nafion/S-graphene composite membrane with electrodes during the making of an MEA. Thereby, the Nafion/S-graphene membrane reduced the PEMFC resistance and increased the power density.

An enhanced mechanical stability and chemical durability were achieved for a Nafion/SGO/CeO_2 composite membrane by Seo *et al.*[142] They reported that the addition of SGO improved the mechanical strength of the composite membrane, while the addition of CeO_2 increased the chemical durability of the composite membrane. Ibrahim *et al.*[143] improved the Nafion membrane for a high-temperature PEMFC by integrating GO into the Nafion matrix. It was demonstrated that by exploiting the Nafion/GO composite membrane, a 20% higher power output was achieved compared to a bare Nafion membrane under both high- and low-temperature conditions. Vinothkannan *et al.*[54] prepared a Nafion/Fe_3O_4-SGO composite membrane and applied it in a high-temperature (120 °C) and low-RH (25%) fuel cell. They reported that the Nafion/Fe_3O_4-SGO membrane could provide reasonable electronic crossover (Fig. 7a) and suppressed H_2 crossover (Fig. 7b). In addition, Fe_3O_4-SGO enabled the Nafion membrane to conduct protons even under anhydrous conditions, which thereby enhanced the proton conductivity of the Nafion/Fe_3O_4-SGO membrane to higher extent at 120 °C under 20% RH. As a consequence, the Nafion/Fe_3O_4-SGO membrane attained the maximum power density of 258 mW cm^{-2}, which was 1.7 fold higher than that of Nafion (144 mW cm^{-2}) (Fig. 7c). The effect of Fe_3O_4-SGO incorporation on the durability of the Nafion membrane was also studied, wherein an extended durability was attained for the Nafion/Fe_3O_4-SGO membrane compared to the pristine Nafion (Fig. 7d).

4.2.2. Nafion/GO or FGO composite membranes for DMFCs. Prapainainar *et al.*[144] utilized silane-grafted GO-mordenite to improve the performance of the Nafion membrane in a DMFC. The power output of the DMFC with the prepared composite membrane was 4 fold better than the Nafion-117 membrane. Wang *et al.*[145] generated proton-transport channels in adenosine triphosphate@graphene oxide Nafion (Nafion/ATP@GO) through an electrostatic layer-by-layer deposition method. Owing to the formation of a well-ordered lamellar structure for ATP and strong hydrogen-bonding interaction between Nafion and GO, the Nafion/ATP@GO membrane exhibited low methanol permeability (2.04×10^{-7} cm^2 s^{-1}) and high proton conductivity (attained 0.345 S cm^{-1} at 80 °C under 100% RH and 0.221 S cm^{-1} at 140 °C under 50% RH). Choi *et al.*[146] synthesized a Nafion/GO composite membrane *via* a solution-casting method and utilized it as an electrolyte in a DMFC. With an optimal loading of 0.2 wt% GO and 5 M methanol concentration, the maximum power density achieved by the Nafion/GO was 141 mW cm^{-2} at 70 °C and 62 mW cm^{-2} at 30 °C. These values were higher than the that of a Nafion 112 membrane under identical operating conditions. The effectual performance of the Nafion/GO membrane regarding a high DMFC efficiency was attributed to the low methanol crossover and improved proton conductivity attained through the amphiphilic nature of GO. To improve the proton conductivity and reduce the methanol crossover of Nafion, Chien *et al.*[147] incorporated sulfonated GO (SGO) into the Nafion matrix by a film-casting technique and the final composite membrane (SGO/Nafion) was used as an electrolyte in a DMFC. The number of charges on the Nafion was enhanced with the acid-functionalized GO, which also enriched the proton conductivity of the composite membrane to a greater extent. Consequently, the power density of the DMFC (using 1 M methanol as fuel) with the SGO/Nafion composite reached 42 mW cm^{-2}, which was 1.2 fold higher than that of the Nafion-115 membrane (33 mW cm^{-2}). A novel bilayer well-aligned Nafion/GO composite membrane was developed *via* a spin-coating method and applied into a direct liquid fuel cell with various fuels, such as methanol, ethanol, and formic acid, by Lue *et al.*[148] They reported that the prepared Nafion/GO composite membrane offered reasonable performance with the aforementioned liquid fuels over the bare Nafion membrane. To obtain highly efficient proton-conducting membranes, Lin *et al.*[149] modified the ionic channels of Nafion 115 by GO papers with the aid of transfer printing followed by a hot-pressing technique. The obtained GO-laminated Nafion 115 composite membrane was then utilized as an electrolyte in a DMFC. The maximum DMFC power density derived for the GO-laminated Nafion 115 composite membrane was 55 mW cm^{-2}, when using 6 M methanol as fuel. The observed performance could be correlated to its immense selectivity to protons achieved by the

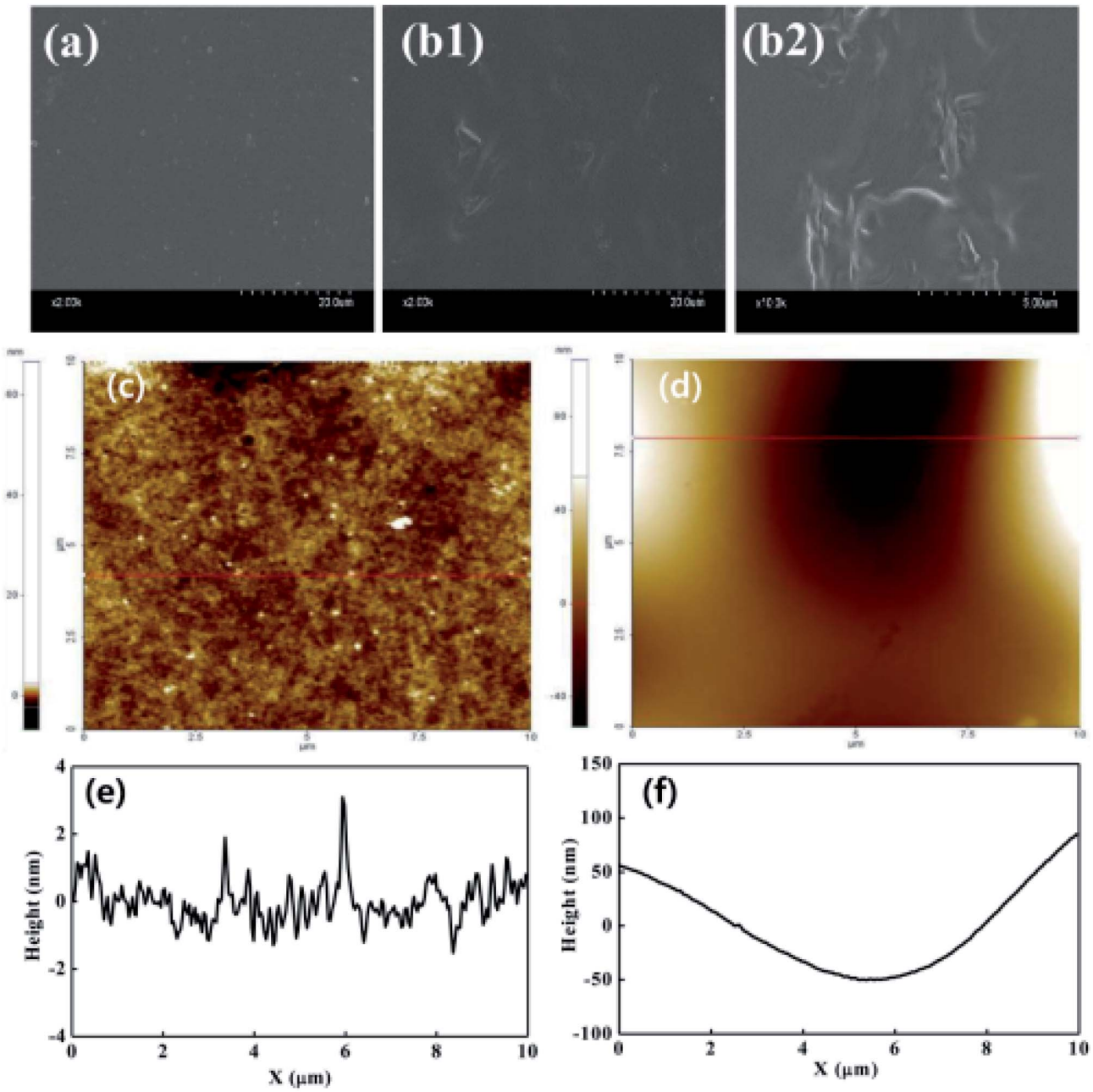

Fig. 6 SEM images of (a) bare Nafion and (b1 and b2) Nafion/S-graphene membranes. AFM images and corresponding line profiles of (c, e) bare Nafion and (d, f) Nafion/S-graphene membranes. Reproduced from ref. 55 with permission from the American Chemical Society, 2016.

parallel orientations of GO sheets within the polymer matrix, as shown in Fig. 8.

Feng *et al.*[150] utilized sulfonated graphene oxide-silica (SGO-SiO_2) as an additive for Nafion to realize a potential electrolyte for DMFCs. The composite membrane was prepared by casting a solution containing a mixture of SGO-SiO_2 and Nafion at 70–120 °C. The introduction of SGO-SiO_2 nanofillers effectively reorganized the conducting channels of Nafion; thereby increasing the proton conductivity and suppressing the methanol permeability of the SGO-SiO_2/Nafion membrane. Fig. 9 exhibits the enhanced transport properties of the SGO-SiO_2/Nafion membrane. From the above, we suggest that the incorporation of SGO-SiO_2 nanofillers is essential to build highly efficient membranes applicable for DMFCs.

The importance of SGO platelets on reducing the methanol permeability and improving the DMFC performance of Nafion/SGO was investigated by Nicotera *et al.*[151] The alignment of exfoliated GO platelets at a preferential orientation in the Nafion matrix provided highly tortuous paths for the diffusion of methanol molecules. However, high water uptake tuning by the Nafion/SGO membrane at high temperature was still guaranteed. Yuan *et al.*[152] developed a poly(diallyldimethylammonium chloride), GO, and Nafion (PDDA/GO/Nafion) composite membrane by a layer-by-layer

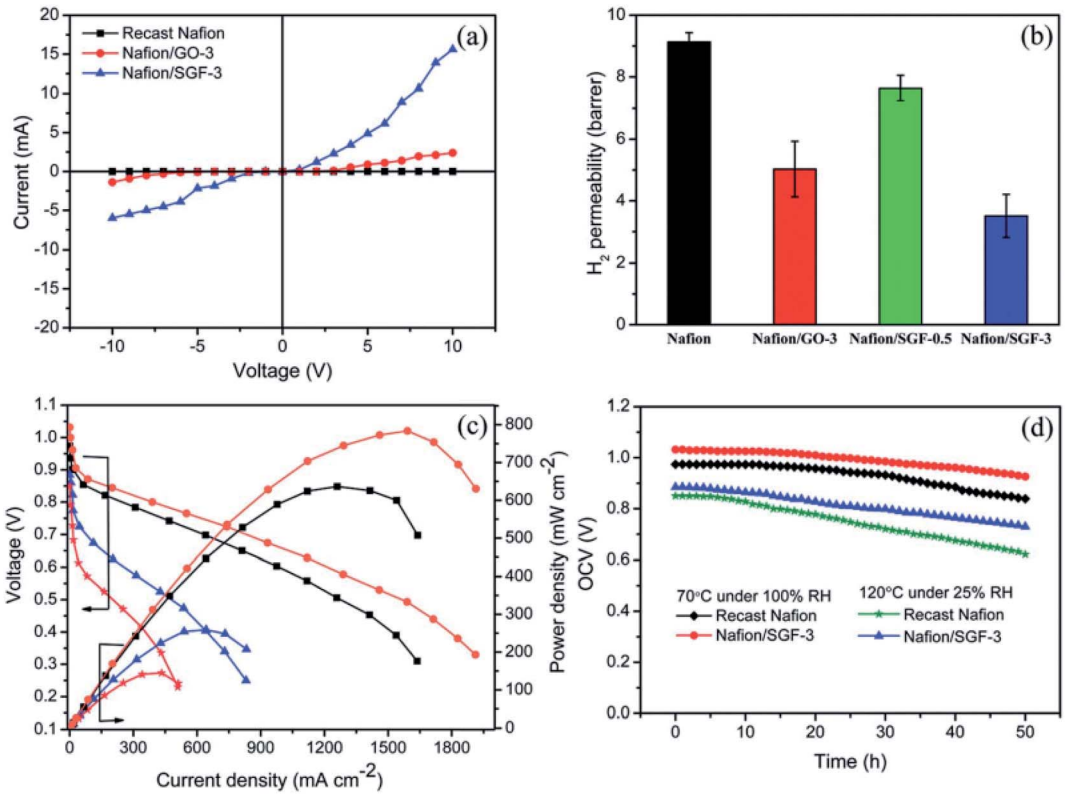

Fig. 7 (a) Current–voltage characteristics of the plain Nafion and composite membranes; (b) H_2 permeability of the plain Nafion and composite membranes; (c) PEMFC performance at 70 °C and 100% RH with black curve = plain Nafion and orange curve = Nafion/Fe_3O_4-SGO membranes and at 120 °C and 25% RH with red curve = plain Nafion and blue curve = Nafion/Fe_3O_4-SGO membranes; (d) durability test of the plain Nafion and Nafion/Fe_3O_4-SGO membranes. Reproduced from ref. 54 published by the Royal Society of Chemistry, 2018.

deposition method, in which PDDA and GO nanosheets were assembled one-by-one onto the surface of Nafion. The prepared PDDA/GO/Nafion membrane was then exploited as an electrolyte in a DMFC. The peak power density achieved by the PDDA/GO/Nafion membrane was 29 mW cm^{-2}, which was about 1.6 times higher than that of pristine Nafion (18 mW cm^{-2}). The obtained maximum power density was related with the suppressed fuel permeability of the composite membrane achieved by the existence of PDDA and GO. Parthiban *et al.*[91] explored S-graphene as a potential filler for the Nafion matrix and applied the Nafion/S-graphene membrane for a DMFC application. The DMFC equipped with Nafion/S-graphene yielded a peak power density of 118 mW cm^{-2} at a load current density of 450 mA cm^{-2}. By comparison, the bare Nafion yielded only 54 mW cm^{-2} at a load current density of 241 mA cm^{-2}. The obtained high DMFC performance of the Nafion/S-graphene membrane was

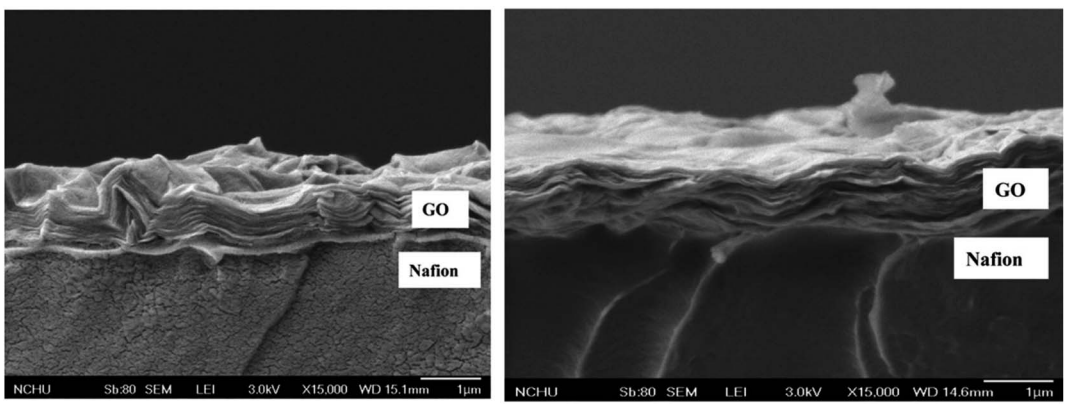

Fig. 8 SEM images of GO-laminated Nafion 115 membranes at different magnitudes: (left) before hot-pressing and (right) after hot-pressing. Reproduced from ref. 149 with permission from Elsevier, 2013.

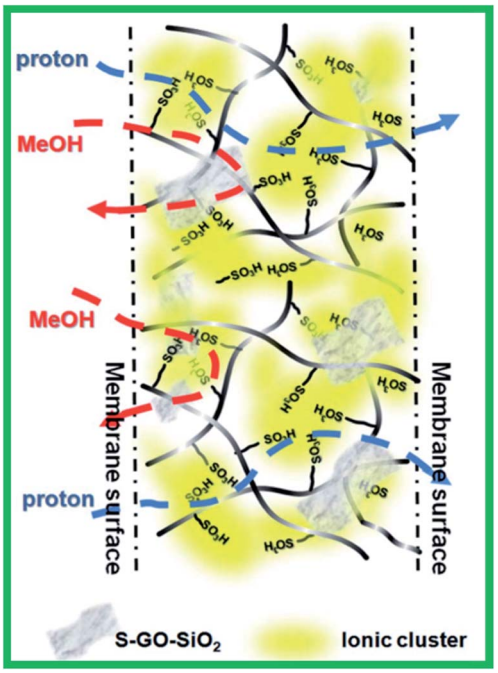

Fig. 9 Schematic illustration of the proton and methanol transports through the SGO-SiO_2/Nafion membrane. Reproduced from ref. 150 with permission from the Royal Society of Chemistry, 2014.

due to the high proton conductivity and restricted methanol crossover across the membrane.

4.3. Fullerene, functionalized fullerene (FF), and other carbon materials for PEMs

Unlike CNT and GO fillers, fullerene and other carbon materials have not yet been so well explored as fillers for state-of-the-art Nafion membranes, owing to their reduced surface area, lack of functionalization methods to disperse them in the Nafion matrices, and bulky nature. Despite these critical issues, several research groups have studied the effect of the incorporation of fullerene, FF, and other carbon materials in Nafion matrices as follows.

4.3.1. Nafion/fullerene, FF, or other carbon materials for PEMFCs and DMFCs. Tasaki *et al.*[153] doped fullerene into Nafion to obtain a proton-conducting hybrid membrane. They observed that under 25% RH, the hybrid membrane took up more water molecules rather than the bare Nafion membrane. So, it could be assumed that the hybrid membrane could produce higher proton conductivity than bare Nafion. The same group improved the dispersibility of hydrophobic fullerene into the Nafion matrix by introducing a new type of dispersant, *i.e.*, poly[tri(ethylene oxide)benzyl]fullerene.[154] So, the essential PEM properties, such as the water uptake and proton conductivity, were enhanced. Postnov *et al.*[155] fabricated a Nafion composite membrane containing fullerene and its water-soluble derivatives, such as tris-malonate-C_{60} and fullerenol-C_{60}. It was found that the integration of these materials into Nafion led to a significant enhancement in proton conductivity under low RH conditions. The functionalization of fullerene and the successful modification of Nafion by functionalized fullerene (FF) was done by Rambabu *et al.*[57] The obtained Nafion/FF was applied as an electrolyte for a DMFC. Among the composite membranes with various wt% of FF, Nafion/FF (1 wt%) exhibited reduced methanol crossover (Fig. 10a) and enhanced DMFC power density (Fig. 10b).

Chai *et al.*[156] prepared a Nafion/carbon nanohybrid membrane *via* a hydrothermal carbonization strategy to utilize as an electrolyte for PEMFCs. Compared with the fuel cell performance of the neat Nafion membrane, the cell equipped with the Nafion/carbon (3.6%) membrane showed an improvement in fuel cell performance of 31.7% at room temperature for a PEMFC, and by 44% for a DMFC operated at 60 °C. Chien *et al.*[157] demonstrated an unprecedented level of water uptake with minimum swelling by embedding activated carbon (AC) into the Nafion matrices. Such a high water uptake with minimal swelling dramatically increased the proton conductivity of the Nafion/AC membrane with low RH. This was accredited to the robust water-retention channels in the composite membrane provided by the AC. The same group studied the PEMFC performance of a Nafion/AC composite membrane under various RH conditions.[158] Under fully hydrated condition, the neat Nafion membrane could achieve a comparable power density to the Nafion/AC composite

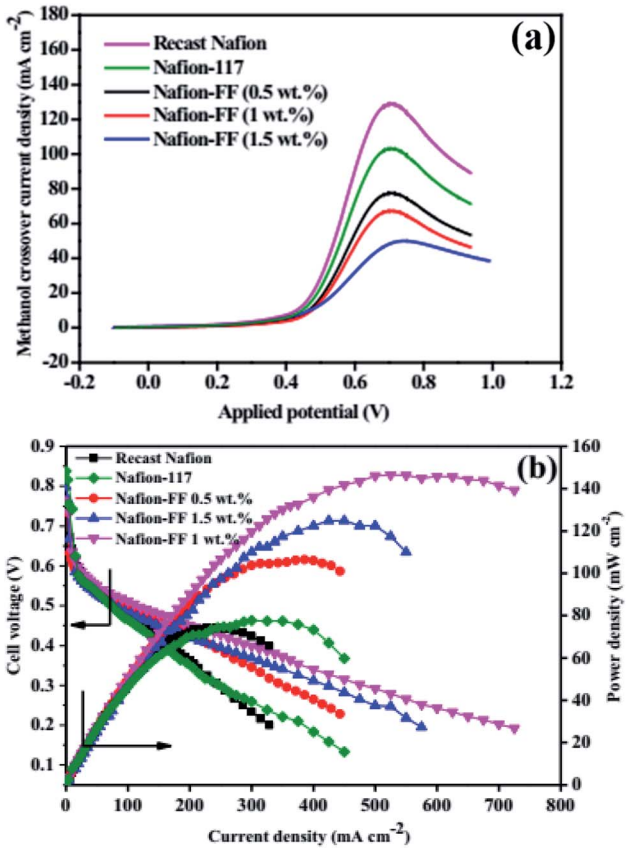

Fig. 10 (a) LSV studies of methanol crossover through the bare Nafion and Nafion/FF composite membranes; (b) DMFC polarization plots of bare Nafion and Nafion/FF composite membranes quantified at 60 °C. Reproduced from ref. 57 with permission from Elsevier, 2016.

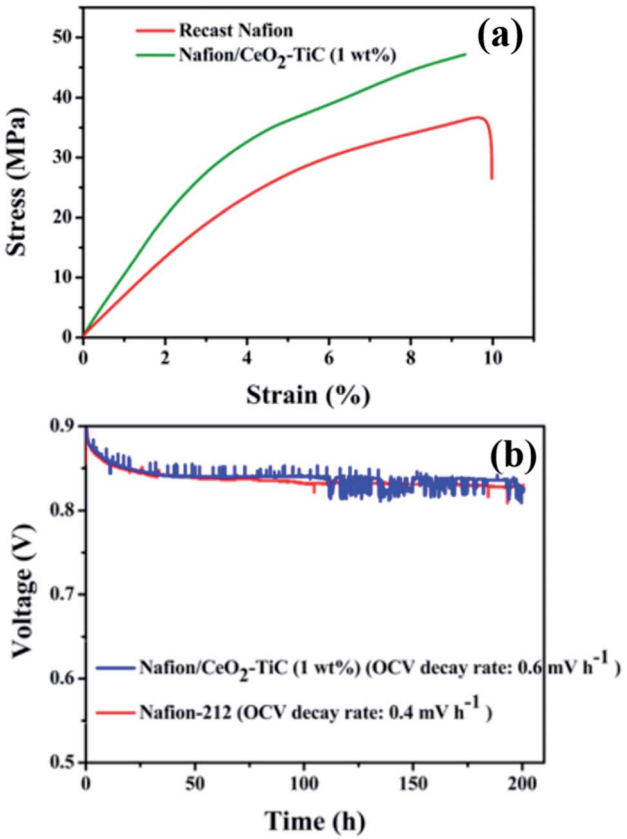

Fig. 11 (a) Stress–strain curves and (b) PEMFC durability curves (quantified at 60 °C and 100% RH) of the Nafion and Nafion/CeO_2–TiC membranes. Reproduced from ref. 74 with permission from the American Chemical Society, 2020.

membrane. However, the power density of neat Nafion was reduced dramatically with reducing the RH, while the Nafion/AC membrane still retained a reasonable power density even under low RH. A porous carbon nanosphere (sPCN) with a number of micropores and pendent $-SO_3H$ groups was synthesized by Guo *et al.*[159] to use as a filler for a Nafion membrane. According to their report, the incorporation of sPCN promoted the T_g mechanical stability, water uptake, and proton conductivity of the Nafion membrane. When applied in a single H_2/O_2 PEMFC, the Nafion/sPCN composite membrane manifested an upper power output of 571 mW cm^{-2}, which was a few times better than the plain Nafion membrane (388 mW cm^{-2}). When, assembling the poly(ethylene glycol) (PEG)-grafted activated carbon (AC-PEG) with Nafion, a largely enhanced water uptake, minimum swelling degree, and higher proton conductivity and H_2/O_2 fuel cell performance were realized for the Nafion/AC-PEG composite membrane.[160] Vinothkannan *et al.*[74] stabilized a CeO_2 radical scavenger in Nafion matrices by using titanium carbide (TiC). The tensile strength (Fig. 11a) and PEMFC durability (Fig. 11b) of the Nafion/CeO_2–TiC membrane were significantly improved, owing to the high mechanical stability of TiC and the radical-scavenging activity of CeO_2. Parthiban *et al.*[92,161,162] integrated different carbon materials, such as nanoporous carbon, sulfonated graphitic carbon nitride, and sulfonated carbon quantum dots, into a Nafion membrane and studied the DMFC properties of the prepared hybrid membranes. Remarkably, the prepared hybrid membranes showed a reduction in methanol crossover and increment in proton conductivity with respect to the neat Nafion membrane. As a result, the hybrid membrane promoted the DMFC power density and durability to a greater extent.

5. Future perspectives

PEMFC is already a developed and well-established technology at the lab scale. However, the widespread commercial adoption of PEMFC, without government incentives, is a challenging task owing to the current inadequate reliability, high cost of auxiliary power units, and durability issues. These problems can be partially minimized by choosing a potential PEM. Up to date, Nafion is the standard and most applied PEM for PEMFCs. Nevertheless, a dramatic decline in proton conductivity at high temperature and low RH and high fuel crossover are important drawbacks of Nafion when applied in fuel cells. Many research efforts are being made to find potential alternatives or to modify the Nafion with appropriate filler materials. The following insights will provide some significant routes for the development of potential Nafion electrolytes for fuel cells. On the one hand, carbon nanomaterials are being widely exploited as potential reinforcing additives for Nafion in order to simultaneously preclude the fuel crossover through Nafion and to enhance the proton conductivity, mechanical integrity, thermal stability, grass transition state, and chemical stability of PEM. Also, the quantity of Nafion is usually lower in the Nafion composite membrane with respect to the bare Nafion membrane, and hence, reduced costs could be expected. Overall, by the proper tuning of the properties of CNs and by optimizing their quantity incorporated into the Nation membrane, they may provide the best solution for the existing problems associated with the state-of the-art Nafion membrane; thereby, advancing the development of PEMFC technologies for global markets. On the other hand, carbon nanomaterials are potential fillers for electrolytes in many other emerging technologies, such as microbial fuel cells, alkaline fuel cells, enzymatic biofuel cells, and vanadium redox flow batteries. Nevertheless, in the pursuit of cost, large-scale production, and dispersion in electrolytes, the additional efforts should be put forward in terms of developing ideal carbon fillers for future electrolytes.

6. Conclusions

The commercial viability of PEMFCs is being widely promoted not only for electricity production but also to address other important issues, such as reducing environmental pollution, alleviating the energy insecurity caused due to the depletion of fossil fuels, and the direct conversion efficiency of fuel to electricity. As an essential component, PEMs underpin the final efficiency of PEMFCs. Even though tremendous efforts have been done on developing potential CNs for the benchmark Nafion PEM, the lack of a collective summary has led to an

unclear understanding of Nafion/CN composite membranes and hindered the futuristic research on CNs for PEMs. Thus, this review intended to afford an overview of the recent advances in promising CNs *i.e.*, CNTs (one-dimensional), GO (two-dimensional), fullerene (zero-dimensional), and other carbon materials, for the Nafion matrix. We also discussed in detail the important requirements for PEMs, such as high thermal stability, glass transition state, mechanical strength, oxidative stability, water-uptake capacity, dimensional stability, IEC, hydration number, self-humidification capability, proton conductivity, and fuel impermeability. In the pursuit of MEAs, currently existing techniques to develop MEAs with the Nafion membrane were discussed. CNs have been proven to be potential fillers to facilitate the aforementioned properties of Nafion, owing to their large surface area and other constructive properties. In addition, the surface functionalization of CNs impart the hydrophilic groups and tune their dispersibility in the Nafion matrix. These functional groups generate new proton-conducting channels at the polymer and filler interface; hence, the functionalization methods for CNs should be chosen carefully for enhanced PEMFC performance and durability.

Conflicts of interest

The authors declare they have no competing financial interests.

Acknowledgements

This work was supported by the Korea Institute of Energy Technology Evaluation and Planning (KETEP) and the Ministry of Trade, Industry & Energy (MOTIE) of the Republic of Korea (No. 20184030202210). This research was supported by Basic Science Research Program through the National Research Foundation of Korea (NRF) funded by the Ministry of Science, ICT and Future Planning (NRF-2020R1A2B5B01001458).

References

1 P. Kallem, N. Yanar and H. Choi, *ACS Sustainable Chem. Eng.*, 2019, **7**, 1808–1825.
2 https://www.eia.gov/totalenergy/data/annual/perspectives.php, 2019 (accessed December 3, 2019).
3 Y. Prykhodko, K. Fatyeyeva, L. Hespel and S. Marais, *Chem. Eng. J.*, 2021, **409**, 127329.
4 https://www.arnhemspeil.nl/nap/dok/2019-01-00-eurostat-report-renewable-energy-statistics-renewable-energy-produced-in-the-eu-increased-by-two-thirds-in-2007-2017%20%282%29.pdf, 2020 (accessed December 3, 2020).
5 O. Ellabban, H. Abu-Rub and F. Blaabjerg, *Renewable Sustainable Energy Rev.*, 2014, **39**, 748–764.
6 S. A. Kalogirou, *Prog. Energy Combust. Sci.*, 2005, **31**, 242–281.
7 D. Gielen, F. Boshell, D. Saygin, M. D. Bazilian, N. Wagner and R. Gorini, *Energy Strategy Rev.*, 2019, **24**, 38–50.
8 S. A. Hashemi, S. Ramakrishna and A. G. Aberle, *Energy Environ. Sci.*, 2020, **13**, 685–743.
9 A. Muzaffar, M. B. Ahamed, K. Deshmukh and J. Thirumalai, *Renewable Sustainable Energy Rev.*, 2019, **101**, 123–145.
10 Y. Wang, K. S. Chen, J. Mishler, S. C. Cho and X. C. Adroher, *Appl. Energy*, 2011, **88**, 981–1007.
11 J. Zhao and X. Li, *Energy Convers. Manage.*, 2019, **199**, 112022.
12 K. Hooshyari, S. Heydari, M. Javanbakht, H. Beydaghi and M. Enhessari, *RSC Adv.*, 2020, **10**, 2709–2721.
13 R. Sandström, J. Ekspong, A. Annamalai, T. Sharifi, A. Klechikov and T. Wågberg, *RSC Adv.*, 2018, **8**, 41566–41574.
14 M. Choi, J. K. Kim, J. Kim, S. Yang, J.-E. Park, O.-H. Kim and Y.-H. Cho, *RSC Adv.*, 2018, **8**, 36313–36322.
15 S. Lu, J. Pan, A. Huang, L. Zhuang and J. Lu, *Proc. Natl. Acad. Sci.*, 2008, **105**, 20611–20614.
16 M. Hemmat Esfe and M. Afrand, *J. Therm. Anal. Calorim.*, 2020, **140**, 1633–1654.
17 S. Giddey, S. P. S. Badwal, A. Kulkarni and C. Munnings, *Prog. Energy Combust. Sci.*, 2012, **38**, 360–399.
18 F. de Bruijn, *Green Chem.*, 2005, **7**, 132–150.
19 W. R. W. Daud, R. E. Rosli, E. H. Majlan, S. A. A. Hamid, R. Mohamed and T. Husaini, *Renewable Energy*, 2017, **113**, 620–638.
20 Z. Zakaria, N. Shaari, S. K. Kamarudin, R. Bahru and M. T. Musa, *Int. J. Energy Res.*, 2020, **44**, 8255–8295.
21 https://www.britannica.com/technology/fuel-cell, 2020 (accessed November 12, 2020).
22 H. A. Elwan, M. Mamlouk and K. Scott, *J. Power Sources*, 2021, **484**, 229197.
23 Y. Chang, Y. Qin, Y. Yin, J. Zhang and X. Li, *Appl. Energy*, 2018, **230**, 643–662.
24 M. A. R. Sadiq Al-Baghdadi, *Int. J. Sustainable Green Energy*, 2007, **26**, 79–90.
25 M. Taufiq Musa, N. Shaari and S. K. Kamarudin, *Int. J. Energy Res.*, 2021, **45**, 1309–1346.
26 D. S. Falcão, V. B. Oliveira, C. M. Rangel, C. Pinho and A. M. F. R. Pinto, *Chem. Eng. Sci.*, 2009, **64**, 2216–2225.
27 M. Díaz, A. Ortiz and I. Ortiz, *J. Membr. Sci.*, 2014, **469**, 379–396.
28 B. Smitha, S. Sridhar and A. A. Khan, *J. Membr. Sci.*, 2005, **259**, 10–26.
29 K. Oh, O. Kwon, B. Son, D. H. Lee and S. Shanmugam, *J. Membr. Sci.*, 2019, **583**, 103–109.
30 K. Ketpang, K. Oh, S.-C. Lim and S. Shanmugam, *J. Power Sources*, 2016, **329**, 441–449.
31 D. Han, S. I. Hossain, B. Son, D. H. Lee and S. Shanmugam, *ACS Sustainable Chem. Eng.*, 2019, **7**, 16889–16899.
32 K. Ketpang, K. Lee and S. Shanmugam, *ACS Appl. Mater. Interfaces*, 2014, **6**, 16734–16744.
33 Y. Zhou, J. Yang, H. Su, J. Zeng, S. P. Jiang and W. A. Goddard, *J. Am. Chem. Soc.*, 2014, **136**, 4954–4964.
34 S. J. Peighambardoust, S. Rowshanzamir and M. Amjadi, *Int. J. Hydrogen Energy*, 2010, **35**, 9349–9384.
35 K. A. Mauritz and R. B. Moore, *Chem. Rev.*, 2004, **104**, 4535–4586.

36 V. Neburchilov, J. Martin, H. Wang and J. Zhang, *J. Power Sources*, 2007, **169**, 221–238.
37 L. Zhang, S.-R. Chae, Z. Hendren, J.-S. Park and M. R. Wiesner, *Chem. Eng. J.*, 2012, **204–206**, 87–97.
38 K. Schmidt-Rohr and Q. Chen, *Nat. Mater.*, 2008, **7**, 75–83.
39 T. Maiyalagan and S. Pasupathi, *Mater. Sci. Forum*, 2010, **657**, 143–189.
40 R. Devanathan, *Energy Environ. Sci.*, 2008, **1**, 101–119.
41 A. K. Sahu, A. Jalajakshi, S. Pitchumani, P. Sridhar and A. K. Shukla, *J. Chem. Sci.*, 2012, **124**, 529–536.
42 V. Parthiban and A. K. Sahu, *New J. Chem.*, 2020, **44**, 7338–7349.
43 M. Vinothkannan, A. R. Kim, K. S. Nahm and D. J. Yoo, *RSC Adv.*, 2016, **6**, 108851–108863.
44 M. Vinothkannan, A. R. Kim, G. Gnana kumar, J.-M. Yoon and D. J. Yoo, *RSC Adv.*, 2017, **7**, 39034–39048.
45 A. R. Kim, M. Vinothkannan and D. J. Yoo, *Int. J. Hydrogen Energy*, 2017, **42**, 4349–4365.
46 A. R. Kim, M. Vinothkannan, M. H. Song, J.-Y. Lee, H.-K. Lee and D. J. Yoo, *Composites, Part B*, 2020, **188**, 107890.
47 A. G. Kumar, A. Singh, H. Komber, B. Voit, B. R. Tiwari, M. T. Noori, M. M. Ghangrekar and S. Banerjee, *ACS Appl. Mater. Interfaces*, 2018, **10**, 14803–14817.
48 J. Han, H. Lee, J. Kim, S. Kim, H. Kim, E. Kim, Y.-E. Sung, K. Kim and J.-C. Lee, *J. Membr. Sci.*, 2020, **612**, 118428.
49 Y. Deng, G. Wang, M. M. Fei, X. Huang, J. Cheng, X. Liu, L. Xing, K. Scott and C. Xu, *RSC Adv.*, 2016, **6**, 72224–72229.
50 X. Xu, L. Li, H. Wang, X. Li and X. Zhuang, *RSC Adv.*, 2015, **5**, 4934–4940.
51 P. Kumar, A. D. Singh, V. Kumar and P. P. Kundu, *RSC Adv.*, 2015, **5**, 63465–63472.
52 N. Wehkamp, M. Breitwieser, A. Büchler, M. Klingele, R. Zengerle and S. Thiele, *RSC Adv.*, 2016, **6**, 24261–24266.
53 M. Martinez, Y. Molmeret, L. Cointeaux, C. Iojoiu, J.-C. Leprêtre, N. El Kissi, P. Judeinstein and J.-Y. Sanchez, *J. Power Sources*, 2010, **195**, 5829–5839.
54 M. Vinothkannan, A. R. Kim, G. Gnana kumar and D. J. Yoo, *RSC Adv.*, 2018, **8**, 7494–7508.
55 A. K. Sahu, K. Ketpang, S. Shanmugam, O. Kwon, S. Lee and H. Kim, *J. Phys. Chem. C*, 2016, **120**, 15855–15866.
56 C. Yin, J. Li, Y. Zhou, H. Zhang, P. Fang and C. He, *ACS Appl. Mater. Interfaces*, 2018, **10**, 14026–14035.
57 G. Rambabu, N. Nagaraju and S. D. Bhat, *Chem. Eng. J.*, 2016, **306**, 43–52.
58 W. Zhou, J. Xiao, Y. Chen, R. Zeng, S. Xiao, H. Nie, F. Li and C. Song, *Polym. Adv. Technol.*, 2011, **22**, 1747–1752.
59 W. Zhang, H. Zheng, C. Zhang, B. Li, F. Fang and Y. Wang, *Ionics*, 2017, **23**, 2103–2112.
60 S. Gahlot and V. Kulshrestha, *ACS Appl. Mater. Interfaces*, 2015, **7**, 264–272.
61 G. Rambabu, S. D. Bhat and F. M. L. Figueiredo, *Nanomaterials*, 2019, **9**, 1292.
62 R. P. Pandey, G. Shukla, M. Manohar and V. K. Shahi, *Adv. Colloid Interface Sci.*, 2017, **240**, 15–30.
63 L. Zhao, Y. Li, H. Zhang, W. Wu, J. Liu and J. Wang, *J. Power Sources*, 2015, **286**, 445–457.
64 L. Vilčiauskas, M. E. Tuckerman, G. Bester, S. J. Paddison and K.-D. Kreuer, *Nat. Chem.*, 2012, **4**, 461–466.
65 Y. Ren, G. H. Chia and Z. Gao, *Nano Today*, 2013, **8**, 577–597.
66 H. Zarrin, D. Higgins, Y. Jun, Z. Chen and M. Fowler, *J. Phys. Chem. C*, 2011, **115**, 20774–20781.
67 V. Di Noto, E. Negro, J.-Y. Sanchez and C. Iojoiu, *J. Am. Chem. Soc.*, 2010, **132**, 2183–2195.
68 I. Nicotera, V. Kosma, C. Simari, S. Angioni, P. Mustarelli and E. Quartarone, *J. Phys. Chem. C*, 2015, **119**, 9745–9753.
69 F. Lu, X. Gao, X. Yan, H. Gao, L. Shi, H. Jia and L. Zheng, *ACS Appl. Mater. Interfaces*, 2013, **5**, 7626–7632.
70 R. Sigwadi, M. S. Dhlamini, T. Mokrani, F. Nemavhola, P. F. Nonjola and P. F. Msomi, *Heliyon*, 2019, **5**, e02240.
71 Y. Fan, D. Tongren and C. J. Cornelius, *Eur. Polym. J.*, 2014, **50**, 271–278.
72 S. Mollá and V. Compañ, *J. Membr. Sci.*, 2011, **372**, 191–200.
73 M. Vinothkannan, R. Hariprasad, S. Ramakrishnan, A. R. Kim and D. J. Yoo, *ACS Sustainable Chem. Eng.*, 2019, **7**, 12847–12857.
74 M. Vinothkannan, S. Ramakrishnan, A. R. Kim, H.-K. Lee and D. J. Yoo, *ACS Appl. Mater. Interfaces*, 2020, **12**, 5704–5716.
75 Y. Devrim, H. Devrim and I. Eroglu, *Int. J. Hydrogen Energy*, 2016, **41**, 10044–10052.
76 A. Ammar, A. M. Al-Enizi, M. A. AlMaadeed and A. Karim, *Arabian J. Chem.*, 2016, **9**, 274–286.
77 A. R. Kim, M. Vinothkannan, C. J. Park and D. J. Yoo, *Polymers*, 2018, **10**, 1346.
78 M. R. de Moura, F. A. Aouada, R. J. Avena-Bustillos, T. H. McHugh, J. M. Krochta and L. H. C. Mattoso, *J. Food Eng.*, 2009, **92**, 448–453.
79 S. Gahlot, H. Gupta, P. K. Jha and V. Kulshrestha, *ACS Omega*, 2017, **2**, 5831–5839.
80 M. J. Parnian, S. Rowshanzamir, A. K. Prasad and S. G. Advani, *J. Membr. Sci.*, 2018, **565**, 342–357.
81 L. Liu, Y. Pu, Y. Lu, N. Li, Z. Hu and S. Chen, *J. Membr. Sci.*, 2021, **621**, 118972.
82 Y.-y. Zhao, E. Tsuchida, Y.-K. Choe, J. Wang, T. Ikeshoji and A. Ohira, *J. Membr. Sci.*, 2015, **487**, 229–239.
83 M. Zatoń, J. Rozière and D. J. Jones, *Sustainable Energy Fuels*, 2017, **1**, 409–438.
84 M. J. Parnian, S. Rowshanzamir, A. K. Prasad and S. G. Advani, *J. Membr. Sci.*, 2018, **556**, 12–22.
85 T. Weissbach, T. J. Peckham and S. Holdcroft, *J. Membr. Sci.*, 2016, **498**, 94–104.
86 X. Liu, Y. Li, J. Xue, W. Zhu, J. Zhang, Y. Yin, Y. Qin, K. Jiao, Q. Du, B. Cheng, X. Zhuang, J. Li and M. D. Guiver, *Nat. Commun.*, 2019, **10**, 842.
87 A. R. Kim, M. Vinothkannan and D. J. Yoo, *J. Energy Chem.*, 2018, **27**, 1247–1260.
88 A. R. Kim, M. Vinothkannan and D. J. Yoo, *Composites, Part B*, 2017, **130**, 103–118.
89 A. M. Baker, L. Wang, W. B. Johnson, A. K. Prasad and S. G. Advani, *J. Phys. Chem. C*, 2014, **118**, 26796–26802.
90 M. A. Aziz and S. Shanmugam, *J. Power Sources*, 2017, **337**, 36–44.

91 V. Parthiban, S. Akula, S. G. Peera, N. Islam and A. K. Sahu, *Energy Fuels*, 2016, **30**, 725–734.
92 P. Velayutham and A. K. Sahu, *J. Phys. Chem. C*, 2018, **122**, 21735–21744.
93 G. Rambabu and S. D. Bhat, *Chem. Eng. J.*, 2014, **243**, 517–525.
94 G. Rambabu and S. D. Bhat, *Electrochim. Acta*, 2015, **176**, 657–669.
95 G. Rambabu, S. Sasikala and S. D. Bhat, *RSC Adv.*, 2016, **6**, 107507–107518.
96 S. Neelakandan, N. K. Jacob, P. Kanagaraj, R. M. Sabarathinam, A. Muthumeenal and A. Nagendran, *RSC Adv.*, 2016, **6**, 51599–51608.
97 S. Neelakandan, P. Kanagaraj, A. Nagendran, D. Rana, T. Matsuura and A. Muthumeenal, *Renewable Energy*, 2015, **78**, 306–313.
98 S. Gahlot, P. P. Sharma, V. Kulshrestha and P. K. Jha, *ACS Appl. Mater. Interfaces*, 2014, **6**, 5595–5601.
99 V. Tricoli and F. Nannetti, *Electrochim. Acta*, 2003, **48**, 2625–2633.
100 E. Chalkovaa, C. Wang, S. Komarneni, J. Lee, M. Fedkin and S. Lvov, *ECS Trans.*, 2019, **25**, 1141–1150.
101 L. Kong, L. Zheng, R. Niu, H. Wang and H. Shi, *RSC Adv.*, 2016, **6**, 100262–100270.
102 H. S. Thiam, W. R. W. Daud, S. K. Kamarudin, A. B. Mohamad, A. A. H. Kadhum, K. S. Loh and E. H. Majlan, *Energy Convers. Manage.*, 2013, **75**, 718–726.
103 H. Ahmad, S. K. Kamarudin, U. A. Hasran and W. R. W. Daud, *Int. J. Hydrogen Energy*, 2011, **36**, 14668–14677.
104 A. Bagheri, M. Javanbakht, H. Beydaghi, P. Salarizadeh, A. Shabanikia and H. Salar Amoli, *RSC Adv.*, 2016, **6**, 39500–39510.
105 S. Mondal, S. Soam and P. P. Kundu, *J. Membr. Sci.*, 2015, **474**, 140–147.
106 R. Thimmappa, M. Gautam, M. C. Devendrachari, A. R. Kottaichamy, Z. M. Bhat, A. Umar and M. O. Thotiyl, *ACS Sustainable Chem. Eng.*, 2019, **7**, 14189–14194.
107 R. P. Ramasamy, in *Encyclopedia of Electrochemical Power Sources*, ed. J. Garche, Elsevier, Amsterdam, 2009, pp. 787–805, DOI: 10.1016/B978-044452745-5.00227-6.
108 J. Choi, J. H. Yeon, S. H. Yook, S. Shin, J. Y. Kim, M. Choi and S. Jang, *ACS Appl. Mater. Interfaces*, 2021, **13**, 806–815.
109 H. I. Kim, M. Wang, S. K. Lee, J. Kang, J.-D. Nam, L. Ci and J. Suhr, *Sci. Rep.*, 2017, **7**, 9512.
110 K. Sarangdevot and B. S. Sonigara, *J. Chem. Pharm. Res.*, 2015, **7**, 916–933.
111 A. Shukla, S. D. Bhat and V. K. Pillai, *J. Membr. Sci.*, 2016, **520**, 657–670.
112 A. R. Kim, J. C. Gabunada and D. J. Yoo, *Int. J. Energy Res.*, 2019, **43**, 2974–2989.
113 S. Mukherjee, A. Bates, S. C. Lee, D.-H. Lee and S. Park, *Int. J. Green Energy*, 2015, **12**, 787–809.
114 W. Zhang, H. Zheng, Z. Chengyi, B. Li, F. Fang and Y. Wang, *Ionics*, 2017, **23**, 2103–2112.
115 M. Ding, X. Ling, D. Yuan, Y. Cheng, C. Wu, Z.-S. Chao, L. Sun, C. Yan and C. Jia, *Front. Chem.*, 2018, **6**, 286.
116 L. Cui, Q. Geng, C. Gong, H. Liu, G. Zheng, G. Wang, Q. Liu and S. Wen, *Polym. Adv. Technol.*, 2015, **26**, 457–464.
117 W.-F. Chen, J.-S. Wu and P.-L. Kuo, *Chem. Mater.*, 2008, **20**, 5756–5767.
118 R. Kannan, B. A. Kakade and V. K. Pillai, *Angew. Chem., Int. Ed.*, 2008, **47**, 2653–2656.
119 R. Kannan, M. Parthasarathy, S. U. Maraveedu, S. Kurungot and V. K. Pillai, *Langmuir*, 2009, **25**, 8299–8305.
120 Y.-H. Liu, B. Yi, Z.-G. Shao, D. Xing and H. Zhang, *Electrochem. Solid-State Lett.*, 2006, **9**, A356.
121 V. Ijeri, L. Cappelletto, S. Bianco, M. Tortello, P. Spinelli and E. Tresso, *J. Membr. Sci.*, 2010, **363**, 265–270.
122 N. Cele, S. Sinha Ray, S. Pillai, O. M. Ndwandwe, S. Nonjola, L. Sikhwivhilu and M. Mathe, *Fuel Cells*, 2010, **10**, 64–71.
123 Y.-L. Liu, Y.-H. Su, C.-M. Chang, Suryani, D.-M. Wang and J.-Y. Lai, *J. Mater. Chem.*, 2010, **20**, 4409–4416.
124 M. Tortello, S. Bianco, V. Ijeri, P. Spinelli and E. Tresso, *J. Membr. Sci.*, 2012, **415–416**, 346–352.
125 N. J. Steffy, V. Parthiban and A. K. Sahu, *J. Membr. Sci.*, 2018, **563**, 65–74.
126 C. Yin, B. Xiong, Q. Liu, J. Li, L. Qian, Y. Zhou and C. He, *J. Membr. Sci.*, 2019, **591**, 117356.
127 G. He, J. Zhao, S. Hu, L. Li, Z. Li, Y. Li, Z. Li, H. Wu, X. Yang and Z. Jiang, *ACS Appl. Mater. Interfaces*, 2014, **6**, 15291–15301.
128 C. Simari, G. Potsi, A. Policicchio, I. Perrotta and I. Nicotera, *J. Phys. Chem. C*, 2016, **120**, 2574–2584.
129 M. Tohidian and S. R. Ghaffarian, *Polym. Adv. Technol.*, 2018, **29**, 1219–1226.
130 J.-M. Thomassin, J. Kollar, G. Caldarella, A. Germain, R. Jérôme and C. Detrembleur, *J. Membr. Sci.*, 2007, **303**, 252–257.
131 M. S. Asgari, M. Nikazar, P. Molla-abbasi and M. M. Hasani-Sadrabadi, *Int. J. Hydrogen Energy*, 2013, **38**, 5894–5902.
132 C.-M. Chang, H.-Y. Li, J.-Y. Lai and Y.-L. Liu, *RSC Adv.*, 2013, **3**, 12895–12904.
133 M. M. Hasani-Sadrabadi, E. Dashtimoghadam, F. S. Majedi, S. Wu, A. Bertsch, H. Moaddel and P. Renaud, *RSC Adv.*, 2013, **3**, 7337–7346.
134 P. Molla-Abbasi, K. Janghorban and M. S. Asgari, *Iran. Polym. J.*, 2018, **27**, 77–86.
135 A. Enotiadis, K. Angjeli, N. Baldino, I. Nicotera and D. Gournis, *Small*, 2012, **8**, 3338–3349.
136 R. Kumar, C. Xu and K. Scott, *RSC Adv.*, 2012, **2**, 8777–8782.
137 B. A. Aragaw, W.-N. Su, J. Rick and B.-J. Hwang, *RSC Adv.*, 2013, **3**, 23212–23221.
138 D. C. Lee, H. N. Yang, S. H. Park and W. J. Kim, *J. Membr. Sci.*, 2014, **452**, 20–28.
139 D. C. Lee, H. N. Yang, S. H. Park, K. W. Park and W. J. Kim, *J. Membr. Sci.*, 2015, **474**, 254–262.
140 A. K. Mishra, N. H. Kim, D. Jung and J. H. Lee, *J. Membr. Sci.*, 2014, **458**, 128–135.
141 Y. Kim, K. Ketpang, S. Jaritphun, J. S. Park and S. Shanmugam, *J. Mater. Chem. A*, 2015, **3**, 8148–8155.
142 D. C. Seo, I. Jeon, E. S. Jeong and J. Y. Jho, *Polymers*, 2020, **12**, 1375.

143 A. Ibrahim, O. Hossain, J. Chaggar, R. Steinberger-Wilckens and A. El-Kharouf, *Int. J. Hydrogen Energy*, 2020, **45**, 5526–5534.
144 P. Prapainainar, N. Pattanapisutkun, C. Prapainainar and P. Kongkachuichay, *Int. J. Hydrogen Energy*, 2019, **44**, 362–378.
145 H. Wang, N. Sun, X. Xu, S. Wang, W. Kang, X. Zhuang, Y. Yin and B. Cheng, *J. Membr. Sci.*, 2021, **620**, 118880.
146 B. G. Choi, Y. S. Huh, Y. C. Park, D. H. Jung, W. H. Hong and H. Park, *Carbon*, 2012, **50**, 5395–5402.
147 H.-C. Chien, L.-D. Tsai, C.-P. Huang, C.-y. Kang, J.-N. Lin and F.-C. Chang, *Int. J. Energy Res.*, 2013, **38**, 13792–13801.
148 S. J. Lue, Y.-L. Pai, C.-M. Shih, M.-C. Wu and S.-M. Lai, *J. Membr. Sci.*, 2015, **493**, 212–223.
149 C. W. Lin and Y. S. Lu, *J. Power Sources*, 2013, **237**, 187–194.
150 K. Feng, B. Tang and P. Wu, *J. Mater. Chem. A*, 2014, **2**, 16083–16092.
151 I. Nicotera, C. Simari, L. Coppola, P. Zygouri, D. Gournis, S. Brutti, F. D. Minuto, A. S. Aricò, D. Sebastian and V. Baglio, *J. Phys. Chem. C*, 2014, **118**, 24357–24368.
152 T. Yuan, L. Pu, Q. Huang, H. Zhang, X. Li and H. Yang, *Electrochim. Acta*, 2014, **117**, 393–397.
153 K. Tasaki, R. DeSousa, H. Wang, J. Gasa, A. Venkatesan, P. Pugazhendhi and R. O. Loutfy, *J. Membr. Sci.*, 2006, **281**, 570–580.
154 K. Tasaki, J. Gasa, H. Wang and R. DeSousa, *Polymer*, 2007, **48**, 4438–4448.
155 D. V. Postnov, V. N. Postnov, I. V. Murin, N. A. Mel'nikova and K. N. Semenov, *Russ. J. Gen. Chem.*, 2016, **86**, 894–896.
156 Z. Chai, C. Wang, H. Zhang, C. M. Doherty, B. P. Ladewig, A. J. Hill and H. Wang, *Adv. Funct. Mater.*, 2010, **20**, 4394–4399.
157 H.-C. Chien, L.-D. Tsai, A. Kelarakis, C.-M. Lai, J.-N. Lin, J. Fang, C.-Y. Zhu and F.-C. Chang, *Polymer*, 2012, **53**, 4927–4930.
158 H.-C. Chien, L.-D. Tsai, C.-M. Lai, J.-N. Lin, C.-Y. Zhu and F.-C. Chang, *J. Power Sources*, 2013, **226**, 87–93.
159 B. Guo, S. W. Tay, Z. Liu and L. Hong, *Int. J. Hydrogen Energy*, 2012, **37**, 14482–14491.
160 L.-D. Tsai, H.-C. Chien, C.-H. Wang, C.-M. Lai, J.-N. Lin, C.-Y. Zhu and F.-C. Chang, *Int. J. Hydrogen Energy*, 2013, **38**, 11331–11339.
161 V. Parthiban, S. Akula and A. K. Sahu, *J. Membr. Sci.*, 2017, **541**, 127–136.
162 V. Parthiban, S. K. Panda and A. K. Sahu, *Electrochim. Acta*, 2018, **292**, 855–864.